Scientific Research Publishing

Journal of Geoscience and Environment Protection, 2024, 12, 115-148
https://www.scirp.org/journal/gep
ISSN Online: 2327-4344
ISSN Print: 2327-4336

Exploring the Relationship between Spatiotemporal Variations in Air Quality and Meteorological Parameters before and during the COVID-19 Pandemic in Xi'an

Muhammad Sajid Mehmood[1,2,3*], Shiyan Zhai[1,2], Gang Li[4,5], Yaochen Qin[1,2], Vithana Pathirannehelage Indika Sandamali Wijeratne[6]

[1]College of Geography and Environmental Science, Henan University, Kaifeng, China
[2]Key Laboratory of Geospatial Technology for Middle and Lower Yellow River Regions, Ministry of Education, Henan University, Kaifeng, China
[3]INTI International University, Persiaran Perdana BBN, Nilai, Malaysia
[4]College of Urban and Environmental Sciences, Northwest University, Xi'an, China
[5]Shaanxi Key Laboratory of Earth Surface System and Environmental Carrying Capacity, Xi'an, China
[6]Department of Geography, University of Colombo, Cumarathunga Munidasa Mawatha, Colombo, Sri Lanka
Email: *m.sajid.mehmood@hotmail.com

How to cite this paper: Mehmood, M. S., Zhai, S. Y., Li, G., Qin, Y. C., & Wijeratne, V. P. I. S. (2024). Exploring the Relationship between Spatiotemporal Variations in Air Quality and Meteorological Parameters before and during the COVID-19 Pandemic in Xi'an. *Journal of Geoscience and Environment Protection, 12,* 115-148.
https://doi.org/10.4236/gep.2024.128007

Received: May 10, 2024
Accepted: August 16, 2024
Published: August 19, 2024

Abstract

The COVID-19 pandemic has significantly changed the air pollution of the world. The present study investigated the temporal and spatial variability in air quality in Xi'an, China, and its relationship with meteorological parameters during and before the COVID-19 pandemic. The outcomes of this study indicated that air pollutants, $PM_{2.5}$, NO_2, PM_{10}, CO, and SO_2 are likely to decrease during winter (25%, 50%, 30%, 40%, and 35%) to spring (30%, 55%, 38%, 50%, and 40%) and summer (40%, 58%, 60%, 55%, and 47%), respectively. However, the concentration of O_3-8h increased by 40%, 55%, and 65% during winter, spring, and summer, respectively. The values of the air quality index decreased during the COVID-19 period. Furthermore, significant positive trends were reported in $PM_{2.5}$, NO_2, PM_{10}, O_3, and SO_2, and no notable trends in CO during the COVID-19 pandemic. Both during and before the COVID-19 period, PM_{10}, NO_2, $PM_{2.5}$, CO, and SO_2 showed a negative correlation with the temperature and a moderately positive significant correlation between O_3-8h and temperature. The findings of this study would help understand the air pollution circumstances in Xi'an before and during the COVID-19 period and offer helpful information regarding the implications of different air pollution control strategies.

Keywords

Spatiotemporal Analysis, Air Quality Index, Meteorological Parameters, COVID-19

1. Introduction

In the 21st century, modernization and industrialization are at the highest point globally, and the risk of air pollution is increasing. Air pollution is one of the biggest threats to public health globally. The low-quality air is causing severe health issues through respiratory diseases, cardiovascular, cancer, intelligence quotient loss, premature mortality, asthma, heart attacks, chronic bronchitis, lung diseases, and shortness of breath (Alqasemi et al., 2021; Rahman et al., 2021). Besides, it has been estimated that 90% of the world's population lives in areas where air pollution levels are above the safe threshold level for human health (WHO, 2016) and that these outcomes are causing about seven million deaths each year and shortening the average life expectancy by about two years (Wyche et al., 2021).

Due to rapid industrialization and uncontrolled population, automobile traffic pressure and the cities' unscrupulous development are increasing daily, resulting in massive amounts of environmental air pollution (Rahman et al., 2021). There are five major air pollutants such as ozone (O_3), nitrogen dioxide (NO_2), sulfur dioxide (SO_2), and particulate matter i.e. $PM_{2.5}$, and PM_{10}, which help in the determination of air quality (Kumari & Toshniwal, 2020). Air quality is severely affected by anthropogenic emissions, and the primary sources of anthropogenic particulate matter emissions are various industries, the transportation sector, and households (Khorsandi et al., 2021). In addition, weather factors are the main determinants of air quality (Kayes et al., 2019; Manju et al., 2018) and are closely interconnected through atmospheric dynamic processes and chemical reactions (Radaideh, 2017). Therefore, air pollution also adversely affects the economy, climate, environment, and vegetation.

The COVID-19 outbreak has had a tremendous influence on society and caused unexpected changes in air quality. Governments all over the world have implemented various policies to promote social distancing, and it is the most efficient strategy to stop the virus's spread (Chinazzi et al., 2020; Kraemer et al., 2020; Sun & Zhai, 2020; Tang et al., 2020; Tian et al., 2020). The Xi'an Municipal Government has also enacted an extreme lockdown from January 25, 2020, which includes the closure of all public transit, restaurants, enterprises, and construction sites. This unexpected quarantine significantly reduced pollutant emissions, offering vital information on the variables that could affect air quality (Pomponi et al., 2020; Tanzer-Gruener et al., 2020).

Recent research indicates that lockdown situations related to the COVID-19 outbreak significantly impact air quality in many cities and nations worldwide. The COVID-19 lockdown affected the world's air quality, and the concentra-

tions of $PM_{2.5}$, NO_2, PM_{10}, CO, and SO_2 decreased while those of O_3 increased during the COVID-19 pandemic (Liu et al., 2021). Many infectious diseases' epidemiological dynamics depend on environmental factors (Shi et al., 2020). Generally, weather indicators can affect virus transmission (Raza et al., 2021). Firstly, Jahangiri et al. (2020) pointed out that temperature is a critical element in the spread of COVID-19. According to Chen et al. (2021), the spread of COVID-19 was also considerably impacted by temperature and humidity. Similarly, Tosepu et al. (2020) analyzed the relationship between weather indicators (rainfall, temperature) and the COVID-19 outbreak in Indonesia and found a significant positive association between COVID-19 and temperature. Furthermore, relative humidity and temperature significantly impact the dissemination of the COVID-19 outbreak in China (Wang & Su, 2020) and affected COVID-19 deaths in Wuhan (Ma et al., 2020; Yao et al., 2021). Few studies have investigated air pollutants' spatial and temporal distribution during the COVID-19 pandemic. For example, Liu et al. (2021) investigated spatiotemporal distribution patterns and variations in air pollution before, during, and after the lockdown. Furthermore, Mehmood et al. (2021) pointed out the spatiotemporal variability of the COVID-19 pandemic concerning socioeconomic factors, climate, and air pollution in Pakistan. They found a significant relationship between humidity and COVID-19 cases.

Some scholars went much more profoundly to analyze the resources of pollutants. They discovered that while transportation and industrial emissions decreased, ozone (O_3) concentrations increased, which implies that emissions from urban activities should be prioritized (Abdullah et al., 2020; Borhani et al., 2021; Dhahad et al., 2021; Islam et al., 2021; Mor et al., 2021; Latif et al., 2021; Wang et al., 2020b; Yang et al., 2020). Eliminating the lockdown of the COVID-19 pandemic at the national level has caused significant changes in air pollution worldwide (Singh et al., 2020). For example, during the COVID-19 pandemic, most of the emissions in Almaty, Kazakhstan, were from residential heating systems and coal power plants rather than vehicles (Kerimray et al., 2020). However, these studies have not examined the complex interplay between the decline in pollutant concentrations and the reduction in emissions during the COVID-19 lockdown. Therefore, this research investigated the connection between climatic variables, air quality, and the COVID-19 pandemic.

Xi'an is located west of the FenWei Plain graben. The Fenhe-Weihe Plain is one of China's most polluted regions due to the high cost of coal, which represents 90% of local energy consumption and is 30% more expensive than the national average. In 2019, the overall air quality in Xi'an was "Unhealthy" with an average US AQI number of 56.6 (WHO, 2021). This area's primary particulate matter (PM) sources include coal consumption, dust emission, industrial activities, lighting, and motor vehicles. Compared to the emission source analysis results of previous years, the proportion of industrial operations declined from 58% to 11.3% in 2020, coal burning decreased from 52% to 18.8%, and motor vehicles increased from 2% to 27.4% (Dai et al., 2018; Wang et al., 2014; Wang et

al., 2019; Wang et al., 2020a). Other research focused on biological and human factors that contribute to O_3 levels. The primary anthropogenic sources of O_3 in Xi'an are industrial emissions, which account for most of the city's O_3 emissions; motor vehicles, which account for most of the city's volatile organic compounds (VOC) emissions (64.4%); organic solvents, and biomass combustion. Various creatures and plants release numerous VOCs in the Qinling Mountain region near Xi'an, which can combine with NOx to produce O_3 in the vicinity of Xi'an (Feng et al., 2016; Li et al., 2018; Sun & Zhai, 2020). Understanding the impact of different human and environmental factors on persistent outbreaks is critical for infection control policymaking, particularly in places where transmission risk is perhaps underestimated, such as wet and warm places. Effective mapping and analysis of city air quality are essential to identify the air quality situation and formulate effective policies (Mahato et al., 2020). These investigations demonstrated the complexities of Xi'an's pollution contributions, but additional research is needed from the viewpoints of geospatial data and urban planning issues.

This research aims to discover the relationships between air quality, the COVID-19 pandemic, and meteorological variables in Xi'an. First, we noticed changes in the COVID-19 distribution from January 2020 to July 2022. Second, we show the meteorological and air quality parameter concentration distribution from 2019 to 2020. We also illustrated how the pollutants were distributed seasonally before and during COVID-19. We used concentrations from the previous full year for a more accurate comparison. We divided them into three seasons (spring, summer, and winter) to correspond to the 12 months of the COVID-19 year. Third, we use R software to conduct a correlation to determine the relationships between air pollutants, COVID-19, and meteorological parameters before and after the COVID-19 period.

2. Data Collection and Methodology

2.1. Stduy Area

Xi'an is the largest city in the central part of Northwest China, and it is the capital of Shaanxi Province. It is located south of the Qinling Mountains, north of the Weihe River, and in the middle of the Guangzhong plain of the Yellow River (Mokoena et al., 2019). The study area is located approximately between geocoordinate 34˚40'0"N, 107˚40'00"E, and 33˚40'0"N, 109˚40'00"E (**Figure 1**). The land extent of Xi'an is 10,097 km^2, with over 8.7 million inhabitants (Mokoena et al., 2019). The climate of the study area is sub-mixed and temperate continental monsoon, and it has a unique model with four seasons each year. The terrain of the study area is primarily flat, and the mountains in the northeast and east are about 1800 meters above sea level. Xi'an, known as Changan in ancient times, is China's most renowned cultural and historical city. It has a severe problem of air pollution and ranks among the top 10 worst cities polluted with air pollutants in China (Cao et al., 2018). The geography and meteorology surrounding Xi'an are

major factors in the poor air quality because of anticyclonic airflows stopping before mountains and leeward slopes, which cause pollutants to collect, and northeasterly winds blowing at low or even zero speeds, which prevent pollutants from dispersing.

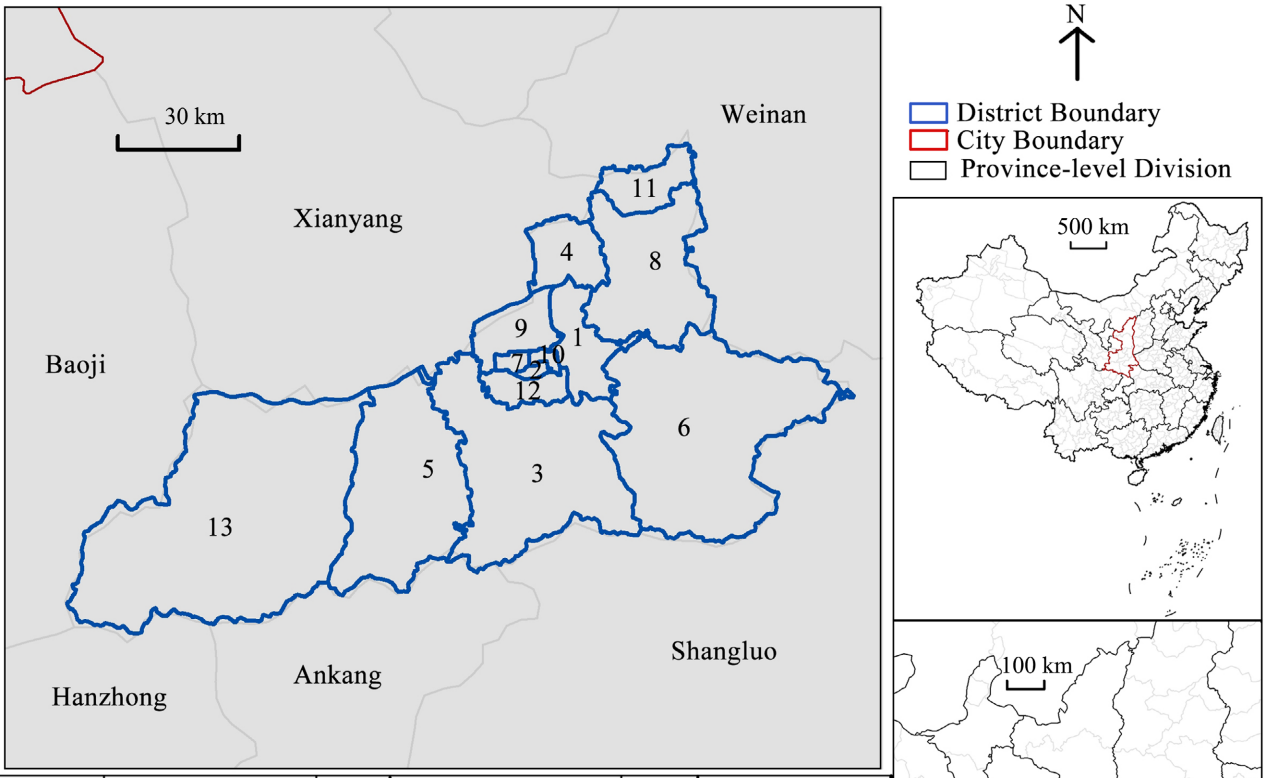

No	District Name	No	District Name	No	District Name
1	Baqiao district	5	Huyi district	9	Weiyang district
2	Beilin district	6	Lantian district	10	Xincheng district
3	Changan district	7	Lianhu district	11	Yanliang district
4	Gaoling district	8	Lintong district	12	Yanta district
				13	Zhouzhi district

Figure 1. Geographic location of Xi'an city in the capital of Shaanxi Province in the central part of Northwest China.

2.2. Data Collection

In this study, two years (2019 and 2020) of daily meteorological parameters (humidity, precipitation, temperature, and wind speed) data from NASA POWER (https://power.larc.nasa.gov/) were used. Data on the daily concentration of air pollutants such as O_3, NO_2, PM_{10}, $PM_{2.5}$, SO_2, CO, and the Air Quality Index, as well as mean values of NO_2, $PM_{2.5}$, PM_{10}, CO, and SO_2, and the 90th percentile concentration of monthly O_3 data were collected from August 2019 to August 2020 using the National Meteorological Information Center (http://www.nmc.cn/). COVID-19 case data was obtained from Xi'an Center for Disease Control and Prevention (http://www.xiancdc.com/). The complete methodology is shown in **Figure 2**.

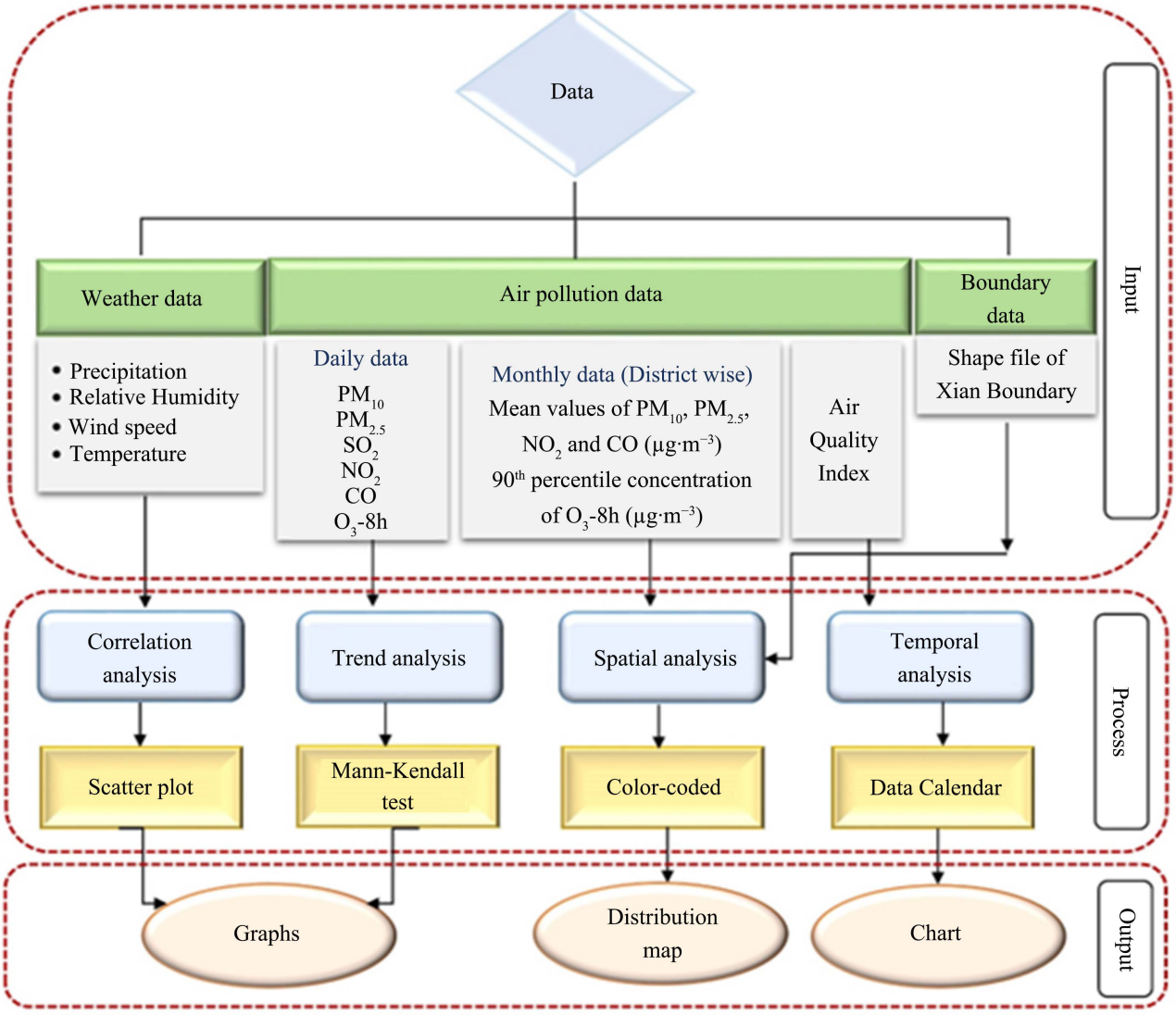

Figure 2. The workflow of data collection, processing, and output in this study.

2.3. Spatial Variability of Air Quality

A geographic information system (GIS) is a robust tool for managing, storing, analyzing, and presenting spatial or geographic data. Under the expert judgment of GIS users or analysts, it can generate remedies to spatial difficulties. Researchers have used GIS technology to investigate pollutants' temporal and spatial distribution (Jensen et al., 2001; Kumar et al., 2016). This study used spatial analysis to detect the spatial distribution patterns of air pollutants in the study area. The data regarding the monthly mean concentration of contaminants, such as NO_2, O_3, PM_{10}, and $PM_{2.5}$ from January to August 2019-20, were analyzed and visualized as a color-coded map regarding their spatial distribution in the study area.

2.4. Temporal Variability and Daily Trend of Air Pollutants

Time series data are ubiquitous, and time series analysis aims to deeply under-

stand the phenomenon, discover repetitive patterns and trends, and predict future trends (van Wijk & van Selow, 1999). This study emphasized determining the temporal characteristics of Air quality index values. For this purpose, daily air quality index data from January 01 to December 31 during 2019-20 were collected. As well as visualized the temporal variation of the air quality index as the data calendar.

2.5. Mann-Kendall Trend Test

This test was used to understand the trend of air pollutants in over 13 districts of Xi'an. Mann-Kendall analysis can be applied to data that are not normally distributed (Meals et al., 2011). The Mann-Kendall analysis assumes that one value can always be declared lower than, greater than, or equal to another: the data are independent; data distribution in the original or converted units remains unchanged. Since Mann-Kendall analysis statistics are not changed to log transformation (test statistics have the same value as the original and log transformation data), it could be applied to many cases. To achieve a Mann-Kendall test, compute the difference between the later-measured value and all earlier-measured values ($Y_j - Y_i$), where $j > i$, and assign the integer value of 1, 0, or −1 to positive differences, no differences, and negative differences, respectively. The test statistic (S) is then computed as the sum of the integers using the following equation.

$$S = \sum_{i=1}^{n=1} \sum_{j=i+1}^{n} \operatorname{sgn}\left(Y_j - Y_i\right) \tag{1}$$

When S is a large positive number, the value measured in the later stage is often larger than that in the early stage and indicates an upward trend (Meals et al., 2011). When S is a large negative number, the later value is often less than the earlier value and indicates a downward trend. No trend will be displayed when the absolute value of S is small. Test statistics τ can be calculated as follows:

$$\tau = \frac{s}{n(n-1)/2} \tag{2}$$

The values of τ range from −1 to +1, similar to the correlation coefficient in regression analysis. When S and τ significantly differ from zero, refuse to deny the null hypothesis of any trend (Meals et al., 2011). If a significant trend is established, the rate of change can be calculated using the Sen Slope estimator (Helsel & Hirsch, 1992; Meals et al., 2011) as given below.

$$\beta_1 = \text{median}\left(\frac{Y_j - Y_i}{X_j - X_i}\right) \tag{3}$$

For all, $i < j$ and $i = 1, 2, \ldots, n-1$ and $j = 2, 3, \ldots, n$; in other words, computing the slope for all pairs of data that were used to calculate S. The median of those slopes is the Sen Slope estimator (Meals et al., 2011).

2.6. Relationship between Weather Parameters and Air Pollutants

A scatter diagram is a tool to analyze the relationship between two variables. One variable is drawn on the vertical axis, and the other is on the horizontal axis. Their interesting point patterns can be displayed graphically concerning patterns (Chow & Yeung, 2006). Using a scatter diagram, this study analyzed the O_3, NO_2, CO, SO_2, $PM_{2.5}$, and PM_{10} with weather indicators such as wind speed, air temperature, precipitation, and relative humidity between January to December 2019 and 2020.

3. Results and Discussions

3.1. Spatio-Temporal Analysis of Air Quality

3.1.1. Spatial Variability of Air Quality over the 13 Districts of Xi'an

To distinguish the spatial distribution pattern of pollutants may include the seasonal component. In this study, the spatial distribution pattern of the pollutants before and during the COVID-19 period was compared during winter (from January to February), spring (from March to May), and summer (from June to August). **Figure 3** illustrates the spatial distribution pattern of air pollutants in the winter season with mean and 90th percentile values of air pollutant concentrations of districts before and during COVID-19. During the winter season (before the COVID-19 period), the highest PM_{10} value i.e. 200.0 to 250.0 $\mu g \cdot m^{-3}$ was reported in Zhoushi District. However, during the COVID-19 winter season, the concentration of PM_{10} was significantly decreased over the study area, and its concentration ranged from 50.0 to 200.0 $\mu g \cdot m^{-3}$.

Similarly, the concentration of NO_2 and $PM_{2.5}$ was significantly decreased during the COVID-19 winter season compared to that recorded before the COVID-19 winter season (**Figure 3**). The reported values during the COVID-19 winter season ranged from 50.0 to 150.0 $\mu g \cdot m^{-3}$ (**Figure 3**). Before COVID-19 in January, the concentration of $PM_{2.5}$ had the highest value ranging from 150.0 to 200.0 $\mu g \cdot m^{-3}$ (**Figure 3**). Earlier, the studies conducted in China revealed a reduction of 29% - 34% and 26% - 48% in the concentration of PM_{10}, and $PM_{2.5}$, respectively, during the COVID-19 period from January to March 2020 compared to that recorded in the same period before COVID-19 (Li et al., 2020).

The concentration of O_3 in Xi'an was distributed evenly both before and during the COVID-19 period in January, with values between 50.0 to 150.0 $\mu g \cdot m^{-3}$. An upward distribution pattern only in February was reported, which has a higher value than before the pandemic, and it varied between 100.0 to 150.0 $\mu g \cdot m^{-3}$ than before the COVID-19 period. In February (before COVID-19), a variation of the distribution of O_3 among all districts of the study area can be identified (**Figure 4**). According to **Figure 4**, Zhouzhi, Lantian, Linton, Yanta, and Xincheng districts reported a concentration of O_3 between 50.0 and 100.0 $\mu g \cdot m^{-3}$. However, the concentration of O_3 was higher during the COVID-19 period than in the previous period i.e. the concentration of O_3 ranged between 100.0 to 150.0 $\mu g \cdot m^{-3}$ for the whole city of Xi'an during the COVID-19 period.

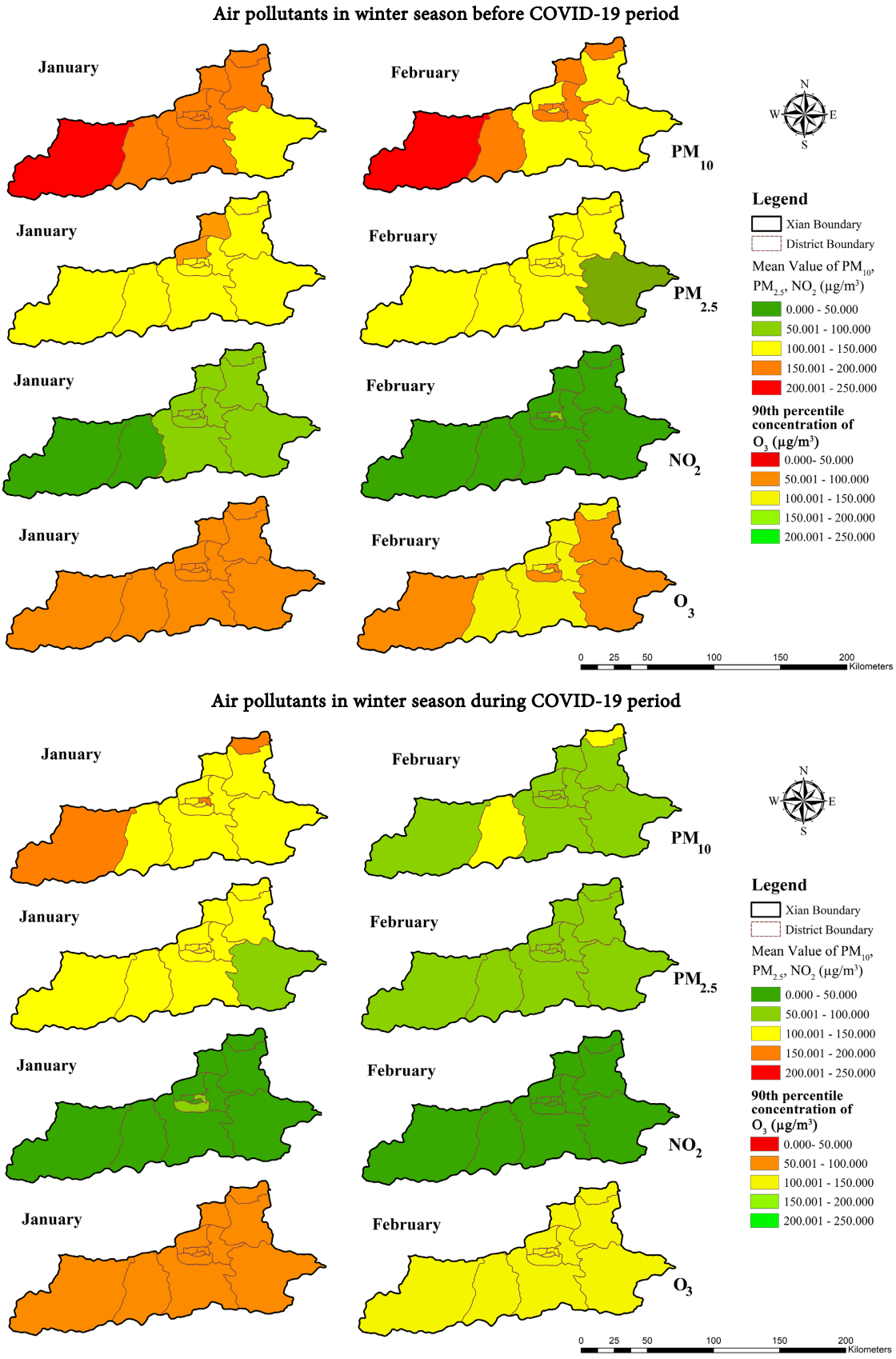

Figure 3. Spatial distribution pattern of air pollutants in winter season before and during COVID-19 period.

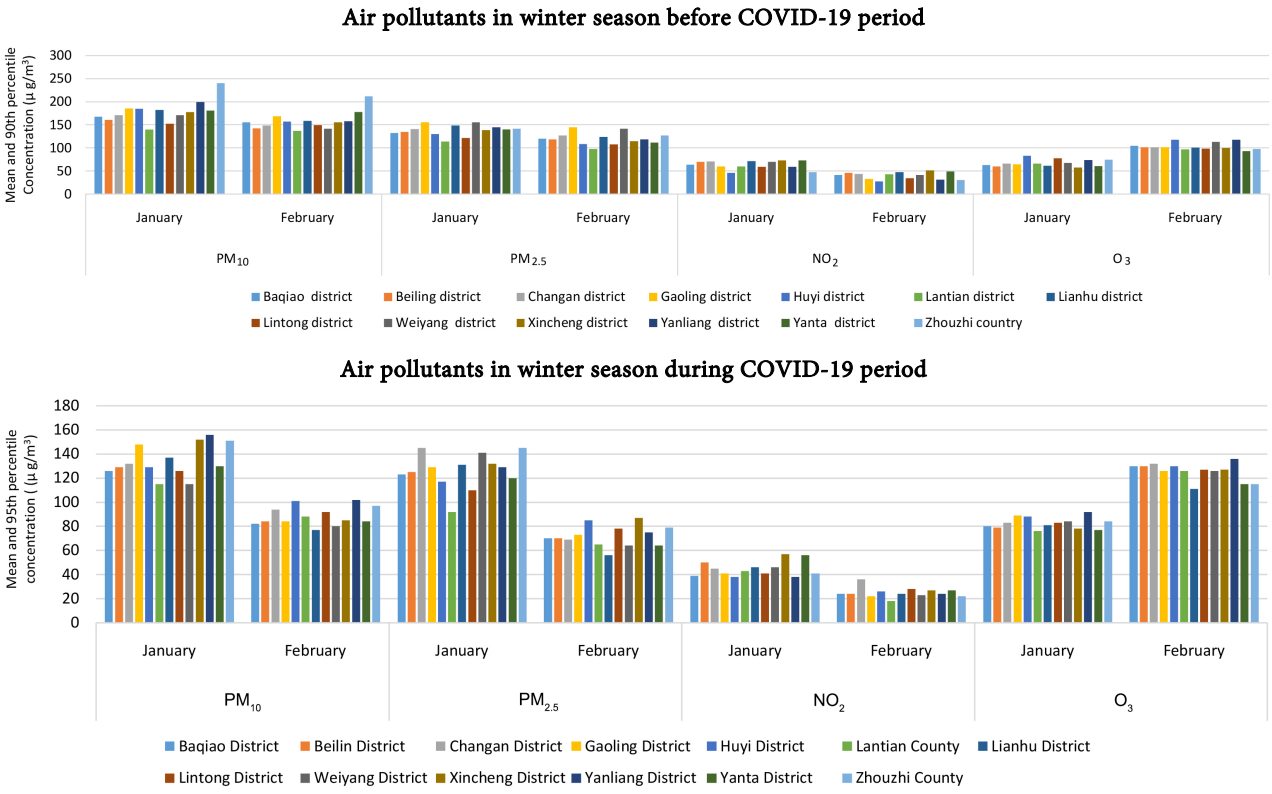

Figure 4. Mean values for PM_{10}, $PM_{2.5}$, and NO_2 concentrations and 90th percentile value of ozone (O_3) concentrations in winter before and during the COVID-19 period.

Figure 5 illustrates the spatial distribution pattern of air pollutants in the district before and during the COVID-19 period in the spring season with their mean and 90th percentile concentration values. In the spring season, the contaminants of PM_{10} fluctuated among all the districts of Xi'an, and values ranged between 50.0 - 150.0 $\mu g \cdot m^{-3}$. During the spring season of 2019, the concentration of PM_{10} ranged from 50.0 to 150.0 $\mu g \cdot m^{-3}$, while lower concentrations were noted before and during the COVID-19 period in the winter season. NO_2 and $PM_{2.5}$ values ranged from 0.001 to 100.0 $\mu g \cdot m^{-3}$, varying from district to district monthly. During May, the lowest NO_2 levels were recorded in all districts, which ranged between 0.001 to 50.0 $\mu g \cdot m^{-3}$. However, the O_3 level showed a steady increase during this season. Accordingly, the highest value of O_3 concentration was recorded in the Huyi district in May, with a value range of 200.0 to 250.0 $\mu g \cdot m^{-3}$. Overall, the distribution of air pollutants decreased in the spring season (before the COVID-19 period) compared to the winter season (before the COVID-19 period).

In the spring season of 2020, the PM_{10} values were evenly distributed over three months, with values ranging from 50.0 to 100.0 $\mu g \cdot m^{-3}$ in all the districts of Xi'an (Figure 5). A significant decrease in PM_{10} concentrations was noted during the COVID-19 spring season. In addition, $PM_{2.5}$ and NO_2 showed a steady decline. It showed the lowest values in districts of Xi'an from the beginning of spring (March) to the end of spring (May). During the last month of the spring

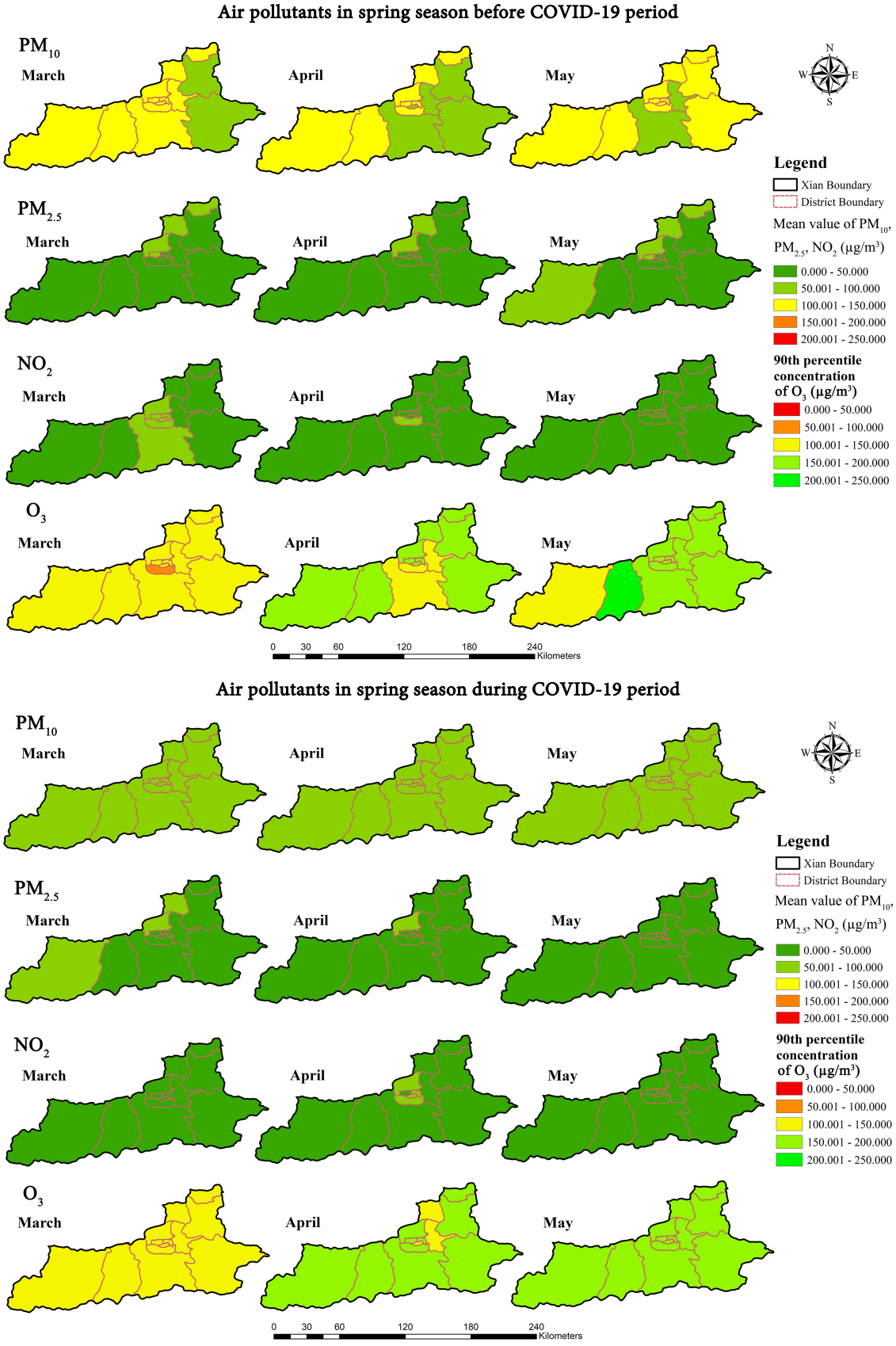

Figure 5. Spatial variation of air pollutants in spring season before and during COVID-19 period.

season i.e. May, the reported values ranged from 0.0 to 50.0 μg·m^{-3} in all districts. However, their levels steadily increased over the months of this season. The highest value of O_3 concentration was recorded during May in Xi'an, with values ranging from 200.0 to 250.0 μg·m^{-3}. The reported values of O_3 concentration were higher than other air pollutants ($PM_{2.5}$ and PM_{10}). Hence, the distribution pattern of air pollutants (NO_2, PM_{10}, and $PM_{2.5}$) showed a decreasing trend during the spring (during the COVID-19 period) compared to that observed during the spring before the COVID-19 period. Figure 6 shows this variability.

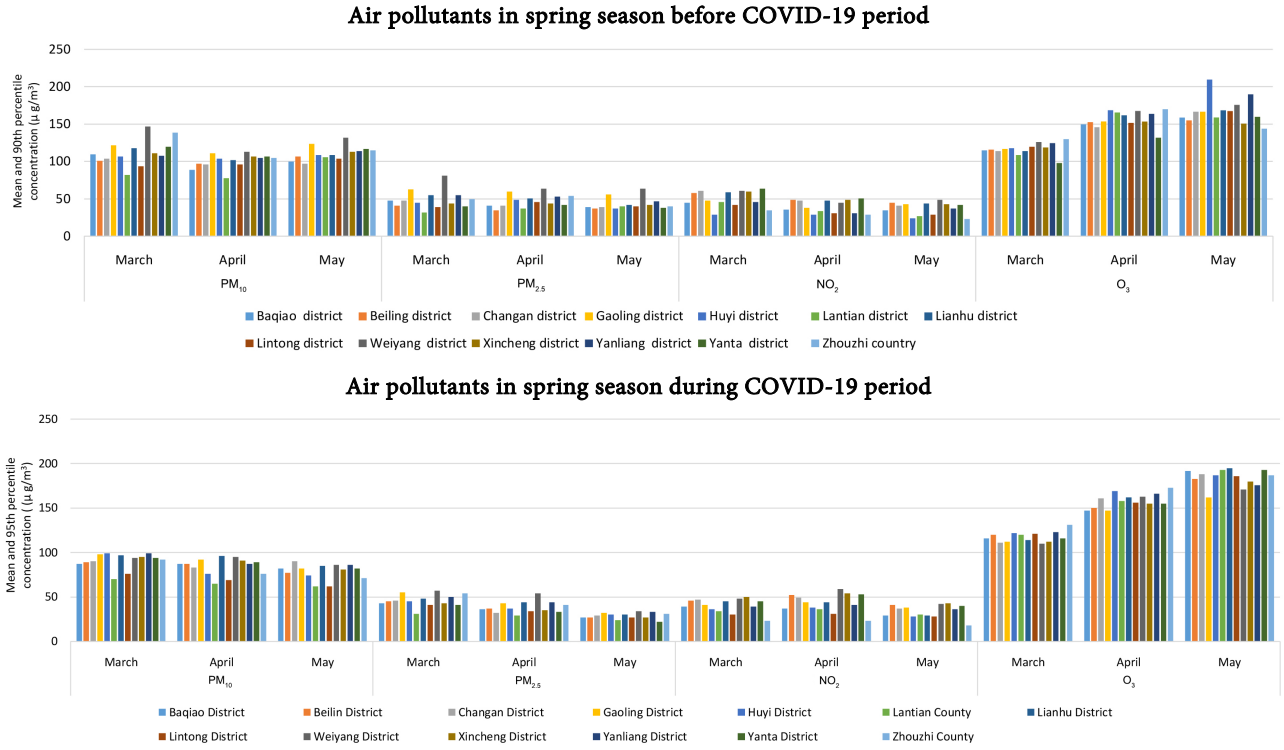

Figure 6. Mean values for PM_{10}, $PM_{2.5}$, and NO_2 concentrations and 90th percentile value of ozone (O_3) concentrations in spring before and during the COVID-19 period.

In the summer, the concentration of studied air pollutants was low compared to other seasons (Figure 7). In the summer of 2019, PM_{10} concentration varied from district to district, ranging from 0.0 to 100.0 μg·m^{-3}. During June, July, and August, PM_{10} spread equally in Zhouzhi, Huyi, and Changan districts with ranges between 0.0 to 50.0 μg·m^{-3}. The highest PM_{10} value was reported from the Yanliang district throughout the summer season before the COVID-19 period. During the summer season (before the COVID-19 period), $PM_{2.5}$ and NO_2 spread throughout all districts in Xi'an without fluctuation, and their concentrations ranged from 0.000 to 50.000 μg·m^{-3} for the whole city of Xi'an (Figure 7). The concentration of O_3 was higher than other air pollutants (PM_{10}, NO_2, and $PM_{2.5}$) during the summer season before the COVID-19 period, and its values ranged from 150.0 to 250.0 μg·m^{-3} (Figure 7). The amount of O_3 also varied from district

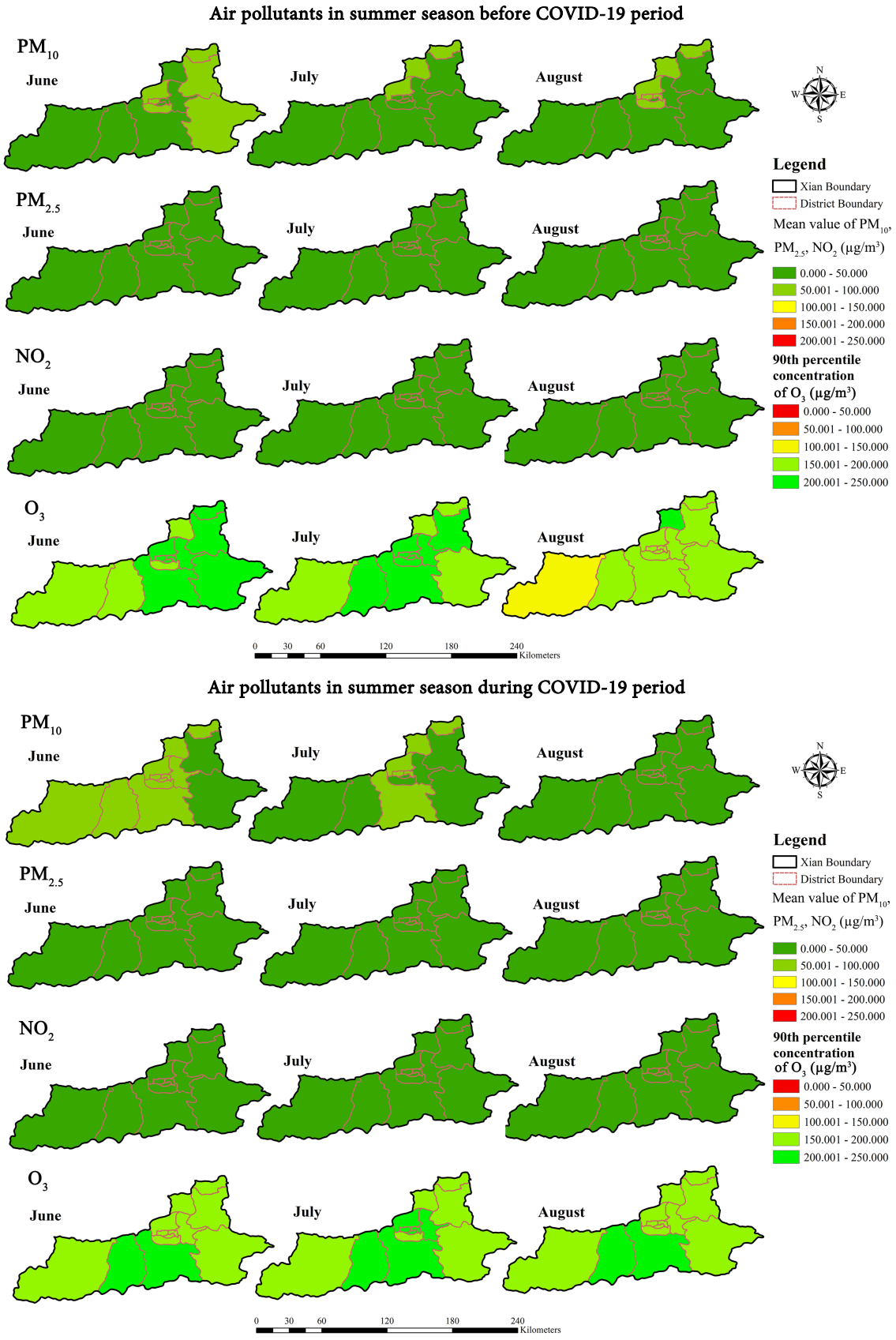

Figure 7. Spatial distribution pattern of air pollutants in summer season before and during COVID-19 period.

to district during this season. In August, a downward distribution pattern in the concentration of O_3 was recorded in the Zhouzhi district, and it ranged from 100.0 to 150.0 μg·m^{-3}.

Figure 7 illustrates that the PM_{10} level declined from the beginning to the end of the summer season during COVID-19. The concentration of PM_{10} ranged from 50.0 to 100.0 μg·m^{-3} during the June 11 districts of the study area. Nevertheless, it was not reported in any district in August, and its concentration ranged from 0.0 to 50.0 μg·m^{-3}. During the COVID-19 period in the summer season, a similar concentration range of $PM_{2.5}$ and NO_2 was recorded. Its spread was uniform throughout all the districts of the study area. The concentration of $PM_{2.5}$ and NO_2 ranged from 0.0 to 50.0 μg·m^{-3} for the whole city of Xi'an during the COVID-19 period. Not only that, but also this distribution pattern was also the same as before the COVID-19 period.

However, the concentration of O_3 in all the districts of Xi'an was higher in the summer than in other seasons, and its values ranged from 200.0 to 250.0 μg·m^{-3} during the COVID-19 period. June and August showed the same distribution pattern of O_3, while the highest O_3 value was recorded in the Huyi and Changan districts during the three months of the summer season. The reported PM_{10}, $PM_{2.5}$, and NO_2 values were lower in summer than in winter and spring seasons. In a similar study, Singh et al. (2020) reported that a decreasing trend in $PM_{2.5}$ can be observed across all regions because of the winter-spring-summer transition. However, the concentration of O_3 was reported to be higher than in other seasons. The bar charts included in Figure 8 showed this variability very clearly.

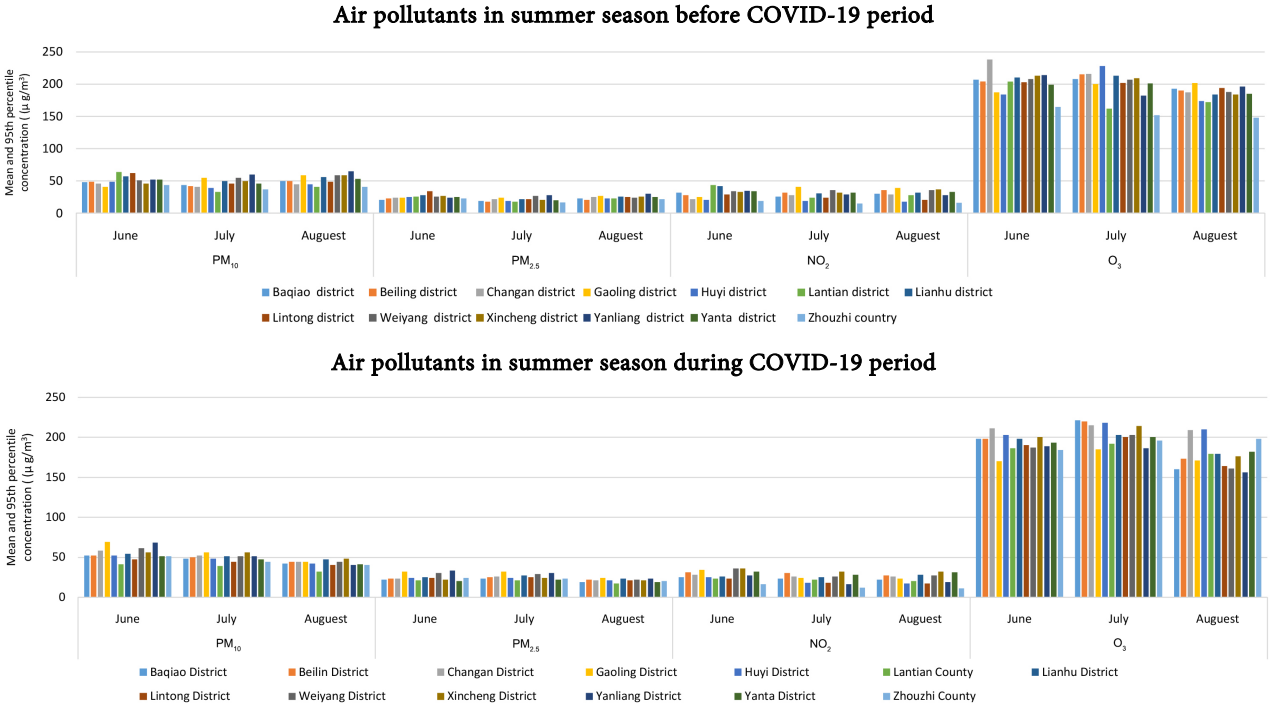

Figure 8. Mean values for PM_{10}, $PM_{2.5}$, and NO_2 concentrations and 90th percentile value of ozone (O_3) concentrations in summer before and during the COVID-19 period.

Air pollutants fluctuate annually, seasonally, monthly, and diurnally in different environments (Singh et al., 2020). Meteorology and local emissions control changes in a specific geographic location. Due to changes in the weather conditions, the primary pollutants emitted during winter to spring and summer may decrease, respectively, while O_3 concentrations tend to increase during the transition from winter, spring, and summer due to photochemical production (Singh et al., 2020). However, some pollutants were highest in other months, possibly due to anthropogenic activities such as transportation, industries, thermal power plants, and residential biomass burning in that area. During the COVID-19 period, the concentration of air pollutants in all the districts showed a significant decrease compared to before the COVID-19 period, which might be due to the reduction of industrial production, strict traffic, and people's lack of willingness to travel, thermal power plants, and residential biomass burning due to the pandemic in the study area. In a similar study, Kumar (2020) applied air quality in India during this COVID-19 period. His conclusion showed that due to the strict lockdown in India, all public transport, industries, and individual activities were shut down, reflected in air quality and aerosols all over India. The aerosols have decreased sharply in India, in contrast to the average value of AOD over the last three years. As well as it's very clear from the plot that the concentration of NO_2 is reduced after the lockdown compared to the three-year average value of NO_2. Finally, they found an apparent reduction in all the pollutants for all cities during the lockdown period.

According to this study, the difference in atmospheric pollutant concentrations during the COVID-19 period and before the COVID-19 period in Xi'an indicates that the emergency response mechanism caused by the COVID-19 pandemic had a significant effect on changing the air pollutant concentration in Xi'an.

3.1.2. Temporal Variability of Air Quality Index (AQI) over the Study Area

The Air Quality Index (AQI) before and during COVID-19 has been visualized through two data calendar maps; one calendar map in 2019 with month and day variation, and the other for 2020 with month and day variation. Daily air quality values have been presented as a calendar map, which is helpful for an intuitive inspection of the severity of pollutants (**Figure 9** and **Figure 10**).

In 2019, before COVID-19, the highest air quality values were recorded compared to those observed in 2020 (**Figure 9**). The pollutant concentrations were extremely high during January, May, and December. These three months had severely polluted days with AQI values of 301 - 500. The lowest AQI was reported during September 2019, with an air quality index of 0 - 50, and it had 11 excellent days. During 2019, around 225 days were excellent/good days (air quality value less than 100) in selected months, and 140 days were polluted with AQI values greater than 101.

Mont / Dat	January	February	March	April	May	June	July	Augest	September	Octomber	November	December
1	215	79	90	100	93	83	116	108	65	77	65	52
2	271	111	54	106	77	85	119	75	94	83	67	79
3	340	87	72	76	71	107	105	37	88	62	79	93
4	296	89	89	67	79	151	96	102	57	35	127	80
5	258	271	87	72	71	42	102	62	111	25	183	103
6	346	216	93	71	57	95	100	40	94	37	158	169
7	230	139	87	112	49	140	123	104	120	50	98	244
8	132	109	71	144	56	153	46	85	110	40	138	190
9	190	133	91	60	85	141	87	44	69	45	189	90
10	201	129	77	74	76	139	102	113	47	45	63	78
11	235	216	62	70	90	95	89	124	39	60	85	105
12	265	235	64	75	481	76	92	89	33	77	80	135
13	287	158	67	58	364	128	140	108	37	75	49	176
14	275	118	60	64	189	118	150	100	32	55	85	149
15	69	135	77	70	107	48	88	120	37	53	99	89
16	65	97	95	81	88	105	56	140	53	49	127	107
17	100	180	94	105	94	54	46	118	40	59	101	82
18	144	202	64	109	86	132	36	123	48	72	95	57
19	104	192	75	114	78	52	51	83	39	90	110	85
20	80	216	120	55	70	38	107	56	45	69	159	175
21	64	170	111	56	90	33	95	50	64	68	183	254
22	103	137	80	65	113	61	42	54	73	90	212	310
23	123	145	78	83	83	108	95	67	70	92	231	319
24	203	195	95	100	123	70	68	136	68	44	38	227
25	99	165	97	141	136	129	144	94	70	53	49	200
26	138	79	107	66	94	105	116	73	78	58	72	55
27	188	98	93	53	61	55	124	43	77	79	95	78
28	159	117	105	69	35	40	79	70	72	95	94	110
29	148	N/A	103	64	44	49	48	103	80	122	114	139
30	130	N/A	72	73	85	91	141	87	88	90	102	66
31	58	N/A	78	N/A	105	N/A	149	77	N/A	90	N/A	70

AQI Value	Description
0 – 50	Excellent
51 – 100	Good
101 – 150	Lightly Polluted
151 – 200	Moderately Polluted
201 – 300	Heavily Polluted
301 – 500	Severely Polluted

Figure 9. Xi'an's air quality index and air quality level before the COVID-19 period (January to December 2019).

Month / Date	January	February	March	April	May	June	July	Augest	September	Octomber	November	December
1	117	185	68	81	99	77	66	67	54	56	76	143
2	149	83	41	50	120	58	136	99	82	30	70	105
3	209	64	52	48	133	93	119	57	84	35	84	48
4	252	127	75	58	145	126	113	74	84	52	112	65
5	152	168	92	72	57	175	137	100	77	54	105	105
6	125	95	110	67	61	95	180	50	82	55	69	134
7	102	99	117	76	36	113	155	30	106	53	81	118
8	149	85	102	70	88	52	115	85	102	53	99	112
9	234	142	110	86	44	36	162	150	72	67	117	120
10	190	134	97	68	64	115	57	120	85	80	140	100
11	130	172	83	59	63	71	43	54	95	83	175	137
12	155	182	93	71	58	75	80	42	81	53	195	166
13	213	172	92	98	78	61	90	80	79	44	162	79
14	118	126	97	79	58	119	41	43	50	35	143	72
15	204	57	77	89	99	59	81	30	69	50	190	104
16	220	45	68	87	70	38	39	30	68	40	152	112
17	247	45	61	97	90	44	42	35	75	68	89	129
18	238	78	78	61	75	116	37	41	72	68	64	72
19	68	92	121	68	66	56	75	46	78	67	69	100
20	80	96	110	77	74	64	85	36	36	70	60	104
21	124	86	96	66	99	61	38	47	33	96	33	149
22	210	87	91	69	124	41	36	52	40	123	37	202
23	277	104	88	74	78	62	48	56	61	103	37	99
24	266	98	82	69	54	135	51	62	65	111	79	81
25	278	158	87	68	77	142	36	98	81	134	68	128
26	201	150	172	63	80	53	90	102	67	104	83	139
27	97	33	34	101	63	40	130	112	59	68	112	205
28	77	48	43	101	88	33	76	107	74	49	109	176
29	87	59	35	97	100	84	90	59	68	64	110	50
30	97	N/A	69	111	95	117	67	35	82	89	130	43
31	155	N/A	58	N/A	115	N/A	101	62	N/A	63	N/A	60

AQI Value	Description
0 – 50	Excellent
51 – 100	Good
101 – 150	Lightly Polluted
151 – 200	Moderately Polluted
201 – 300	Heavily Polluted
301 – 500	Severely Polluted
	No data

Figure 10. Xi'an's air quality index and air quality level of Xian, during the COVID-19 period (January to December 2020).

Figure 10 illustrates that pollutant concentrations were extremely high during January and December 2020, but it did not include severely polluted days as the

AQI values were not greater than 300. The lowest air quality index was reported for August, with an air quality value of 0 - 50, and it has 11 excellent days. Not only that but no day in 2020 that was severely polluted was also reported in all the months. In 2020, 250 days can be identified as excellent/good days with air quality values less than 100 in the selected months, and 116 days were polluted with AQI values greater than 101.

According to **Figure 9** and **Figure 10**, sixteen more excellent days were reported during COVID-19 in 2020 compared to before COVID-19 in 2019, which was 41% more than in 2019. Ten more good days were reported during COVID-19 in 2020 than in 2019. Air quality levels of heavy pollution days decreased in 2020 and 2019 by 31.8%, and eleven lightly polluted days decreased in 2020 compared to 2019. Hence, no severely polluted days were reported in 2020, and air quality was 100% decreased, which was a good sign for the environment during COVID-19. In a similar study, Mahato et al. (2020) documented that stated earlier the lockdown started on the 24th of March, and just after 1 day of the beginning of the lockdown (i.e. 25th of March), there was a significant upgrade in air quality in comparison to that of the pre-lockdown phase in New Delhi, India. There are several reasons behind the variations in air quality indices of the study area during the pre-and-post COVID-19 period. Xi'an is the largest city and the provincial capital in Central China. It is one of the most attractive places for tourists in China and has a market and trade center. Hence, it has rapid urbanization, a high population growth rate, and increasing traffic volume daily. The above factors led to increasing the pollution indices before the COVID-19 period. During the COVID-19 period, Xi'an restricted most of its economic and human activities, except for the utilities of primary products and facilities such as health, food, medicine, human and animal well-being, banks, families, public transport, construction, and emergency services, and energy (electricity and fuel). As a result, the primary source of emissions changed to a low level. Not only that, but the metrological conditions lead to a change in air pollution indices. For example, heavy and severe pollution days increased more in the winter (December, January, and February) than in other seasons before and during COVID-19. The researchers observed similar changes regarding air quality in different countries (Gouda et al., 2021; Khorsandi et al., 2021). Overall, the COVID-19 period leads to comparatively healthier air quality than before the COVID-19 period.

3.1.3. Daily Trend of Air Pollutants over the Study Area

To examine the trends (decreasing or increasing) of air pollutants' variation over time, Mann-Kendall's (M. K.) trend analysis was performed in this study. **Figure 11** represents the Mann-Kendall test results for the daily $PM_{2.5}$, PM_{10}, NO_2, SO_2, CO, O_3-8h ($\mu g \cdot m^{-3}$) in Xi'an from January 01 to December 31, 2019 (before the COVID-19 period) and January 01 to December 31, 2020 (during COVID-19 period).

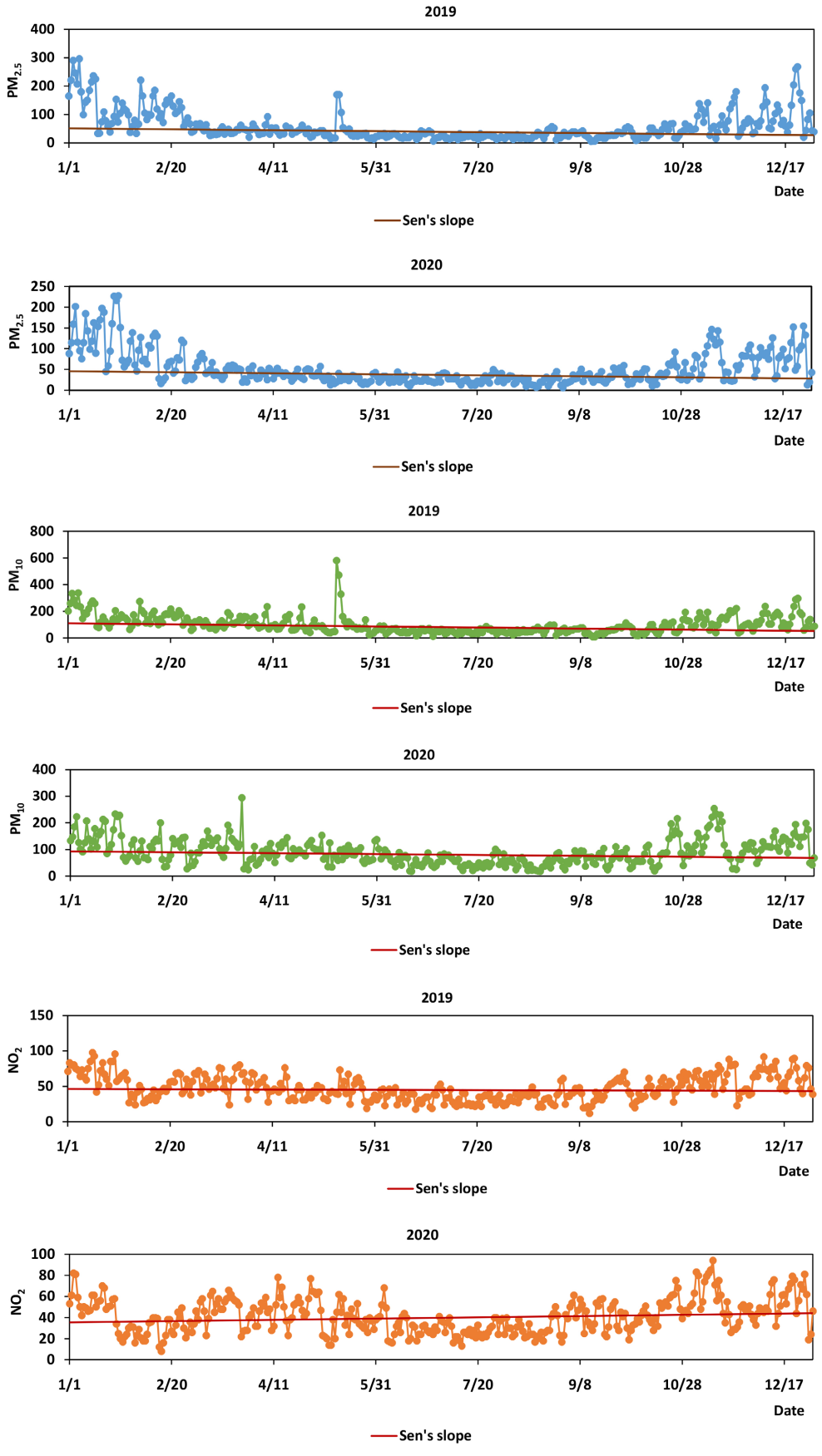
2019
PM2.5
400
300
200
100
0
1/1
2/20
4/11
5/31
7/20
9/8
10/28
12/17
Date
Sen's slope
2020
PM2.5
250
200
150
100
50
0
1/1
2/20
4/11
5/31
7/20
9/8
10/28
12/17
Date
Sen's slope
2019
PM10
800
600
400
200
0
1/1
2/20
4/11
5/31
7/20
9/8
10/28
12/17
Date
Sen's slope
2020
PM10
400
300
200
100
0
1/1
2/20
4/11
5/31
7/20
9/8
10/28
12/17
Date
Sen's slope
2019
NO2
150
100
50
0
1/1
2/20
4/11
5/31
7/20
9/8
10/28
12/17
Date
Sen's slope
2020
NO2
100
80
60
40
20
0
1/1
2/20
4/11
5/31
7/20
9/8
10/28
12/17
Date
Sen's slope

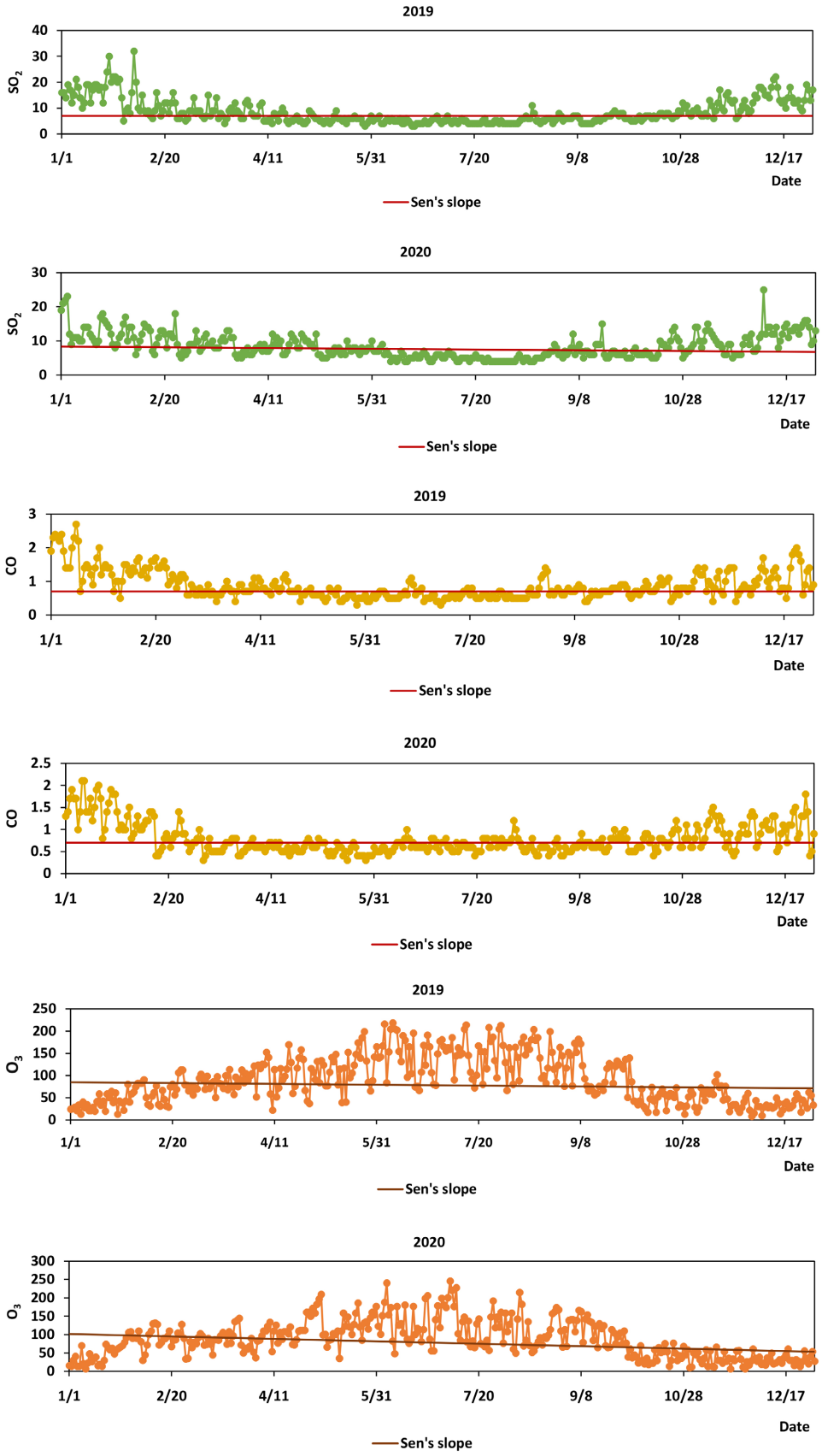

Figure 11. Daily $PM_{2.5}$, PM_{10}, NO_2, SO_2, CO, O_3-8h ($\mu g \cdot m^{-3}$) before COVID-19 and during the COVID-19 period.

In the Mann-Kendall analysis of air pollution data, the overall results of the M. K. trend analysis are presented in **Table 1**. If the *p*-value was less than the significance level i.e. α = 0.05, H0 was rejected. Rejecting H0 indicates a trend in the time series while accepting H0 indicates no trend was detected. When rejecting the null hypothesis, the results have been said to be statistically significant.

Table 1. Summary of results in Mann Kendall Test-before COVID-19 period.

Air pollutants	Mann-Kendall Statistic (S)	Kendall's Tau	Var (S)	*p*-value at α = 0.05 (two tailed test)	Test Clarification
Mann Kendall Test Results-2019					
$PM_{2.5}$	−9391.0	−0.142	5423253.67	<0.0001	H_0 = Reject
PM_{10}	−12512.0	−0.189	5424592.00	<0.0001	H_0 = Reject
NO_2	−2134.0	−0.032	5422440.67	0.360	H_0 = Accept
SO_2	−1747.0	−0.028	5353320.33	0.450	H_0 = Accept
CO	−5922.0	−0.094	5345195.33	0.010	H_0 = Reject
O_3-8h	−3536.0	−0.053	5424514.67	0.129	H_0 = Accept
Mann Kendall Test Results-2020					
$PM_{2.5}$	−7943.0	−0.142	5423253.67	<0.0001	H_0 = Reject
PM_{10}	−12512.0	−0.189	5424592.00	<0.0001	H_0 = Reject
NO_2	−2134.0	0.098	5421663.33	0.006	H_0 = Reject
SO_2	−7477.0	−0.118	5360057.00	0.001	H_0 = Reject
CO	643.0	0.010	5314985.00	0.781	H_0 = Accept
O_3-8h	−11663.0	−0.176	5424219.00	<0.0001	H_0 = Reject

H0 = There is no trend in the study period.

H1 = There is a trend in the study period.

The M. K. test gave fascinating insights into air pollutants data before and during COVID-19. The M. K. test Statistic (S) indicated a decreased trend for the five air pollutants such as $PM_{2.5}$, PM_{10}, NO_2, SO_2, CO, and O_3-8h before COVID-19 (**Table 1**). However, an increasing trend in O_3-8h and NO_2 air pollutants was recorded during COVID-19. The null hypothesis (H0) was rejected for $PM_{2.5}$, PM_{10}, and CO air pollutants before the COVID-19 period, while it was accepted for the pollutants i.e. O_3-8h, NO_2, and SO_2 before the COVID-19 period. This trend suggests that a significant decreasing trend can be identified for $PM_{2.5}$, PM_{10}, and CO, and no trend was identified for O_3-8h, NO_2, and SO_2 before COVID-19. During the COVID-19 period 2020, the null hypothesis (H0) was rejected for $PM_{2.5}$, PM_{10}, NO_2, SO_2, and O_3-8h while it was accepted for CO only. This suggests that a significant decreasing trend can be identified for $PM_{2.5}$,

PM_{10}, NO_2, SO_2, and O_3-8h, with no significant trend for CO during the COVID-19 period. Among the pollutants, the concentrations of five major pollutants showed a decreasing trend. In contrast, CO had no significant trend during the COVID-19 period.

3.2. Relationship between Weather Parameters and Air Pollutants in the Study Area before and during the COVID-19 Pandemic

The scatter plot method was applied to study the relationship between the weather and air pollutants data from January to December 2019 and 2020 (Figures 12-15). The details about each relationship are given below:

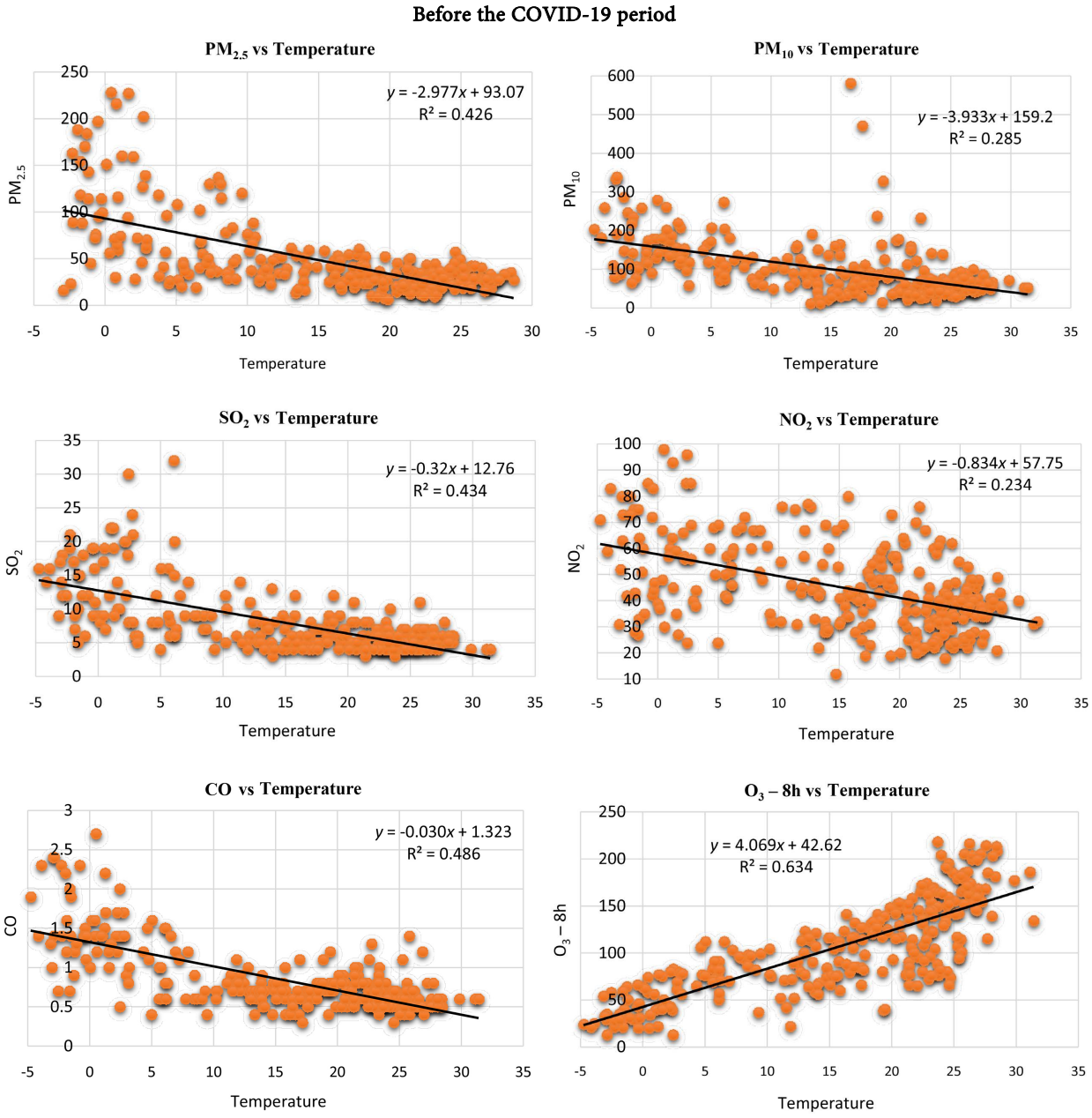

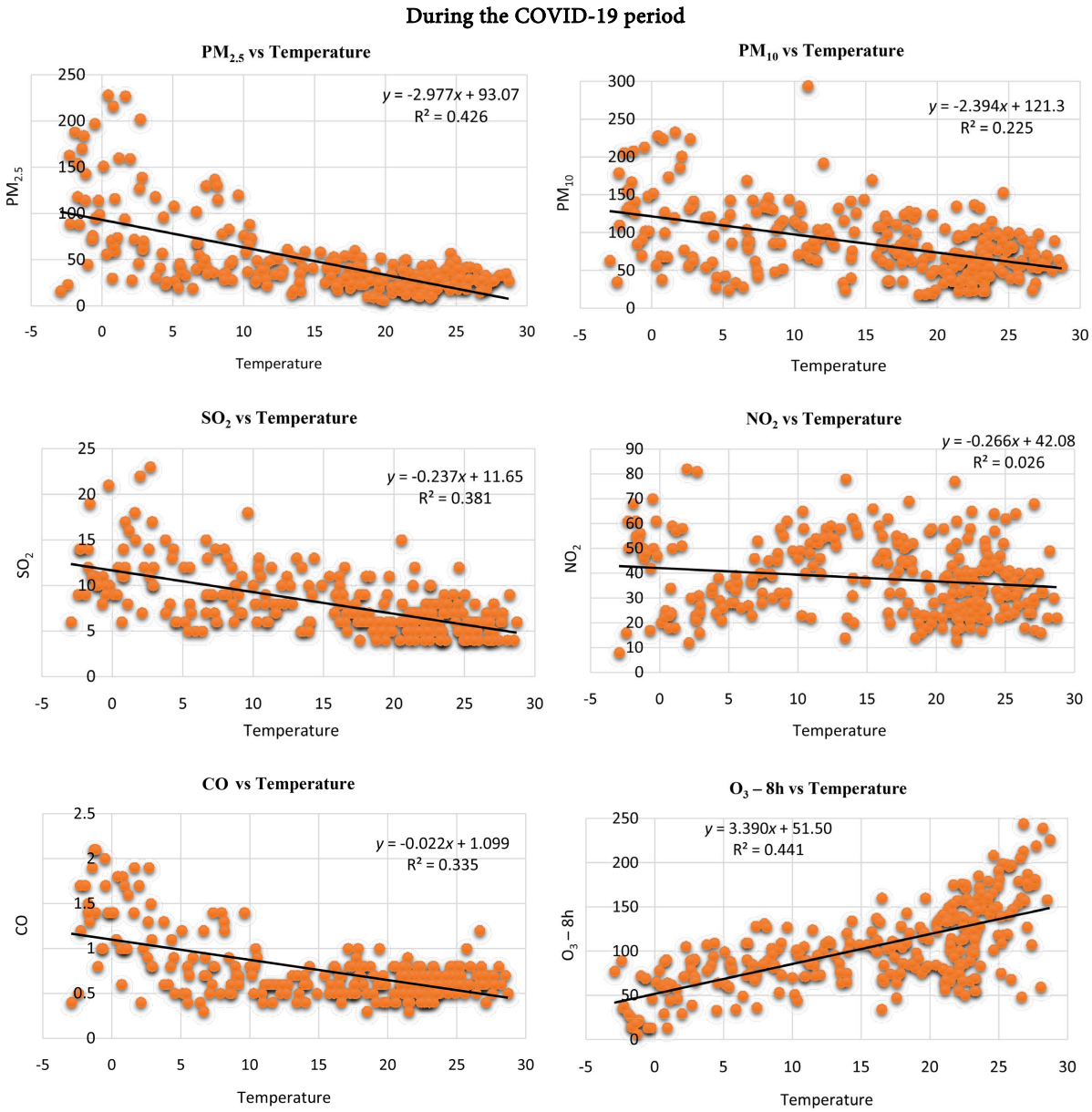

Figure 12. The relationship between air pollutant and temperature before and during the COVID-19 period.

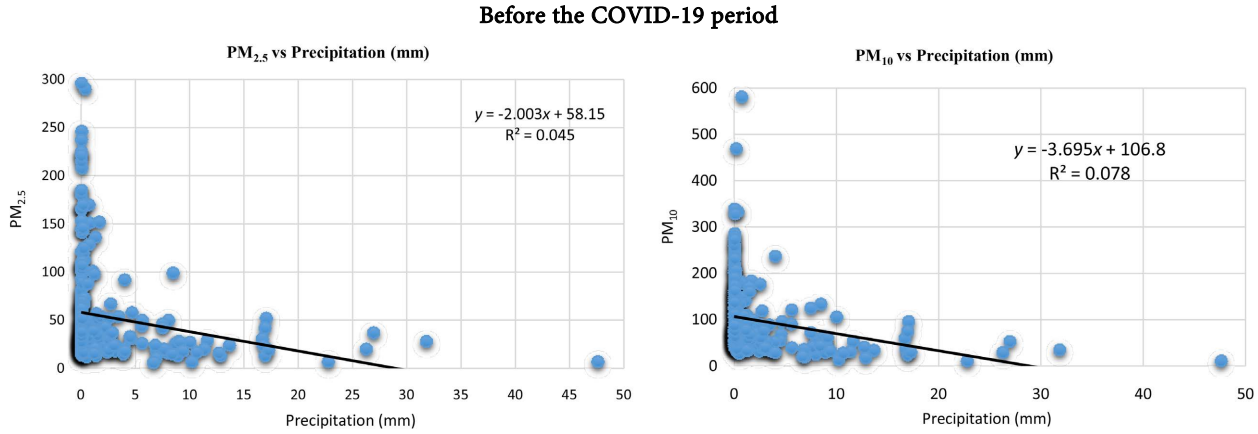

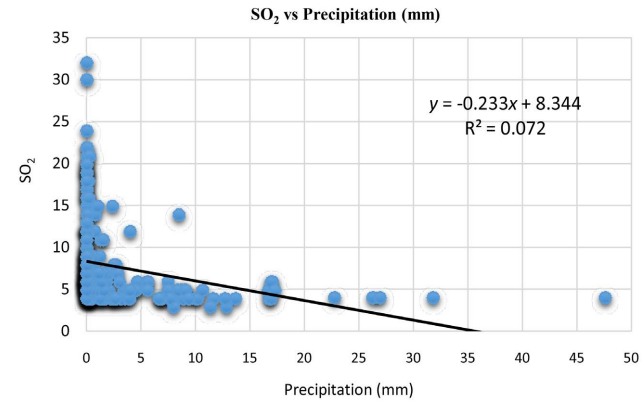

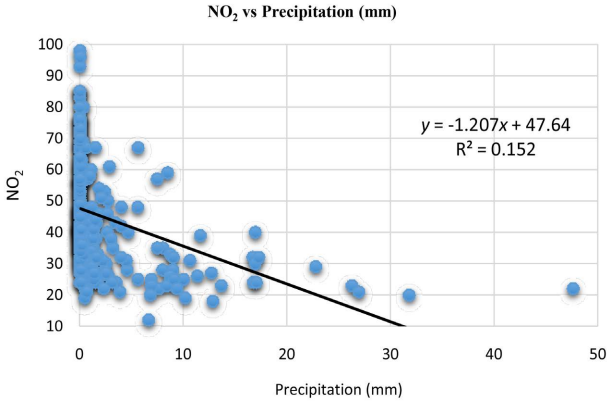

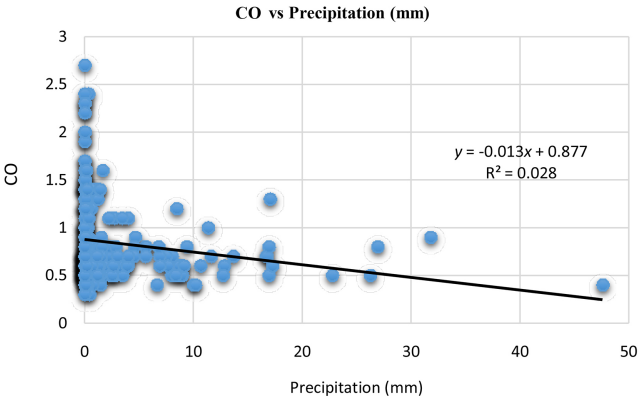

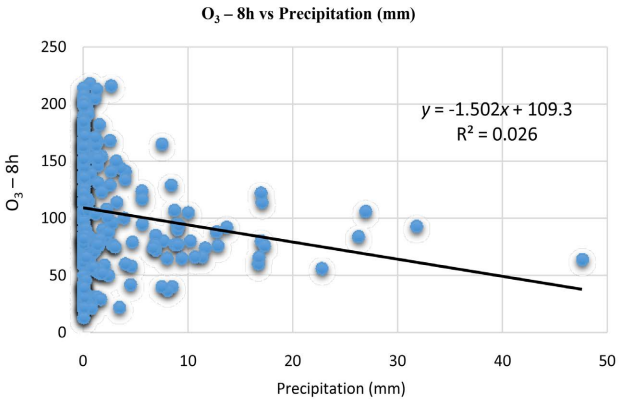

During the COVID-19 period

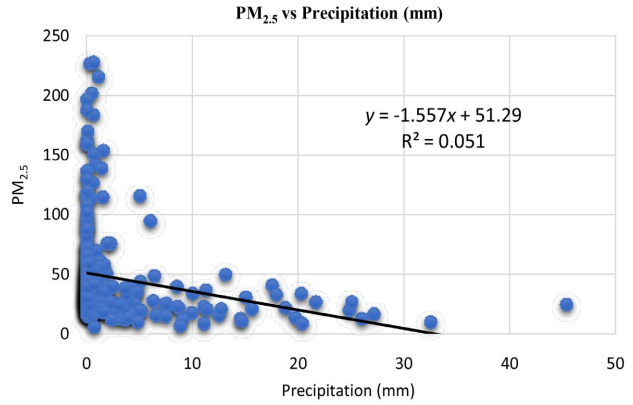

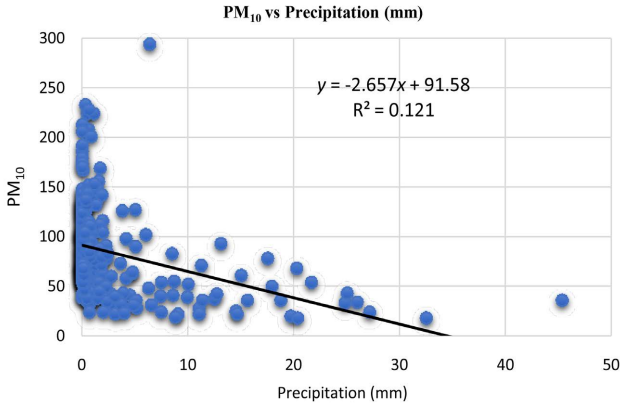

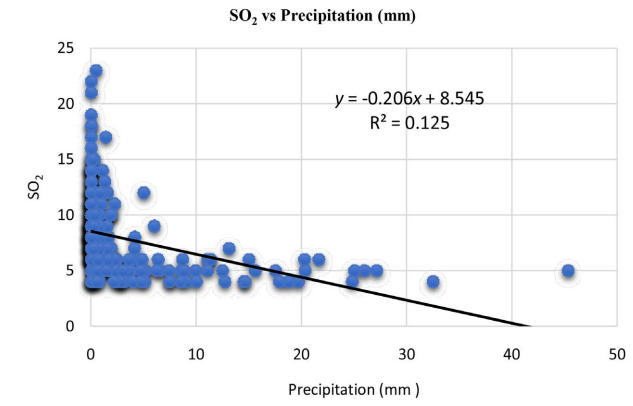

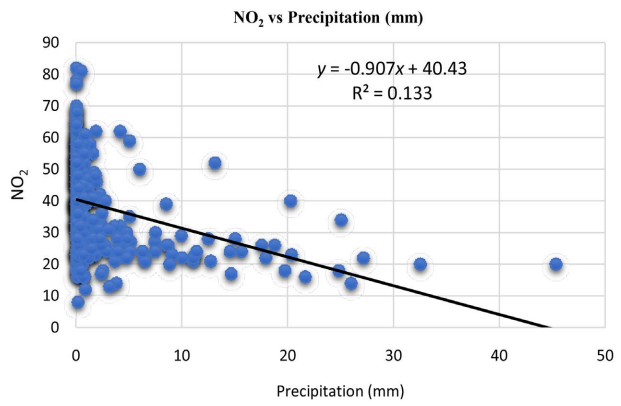

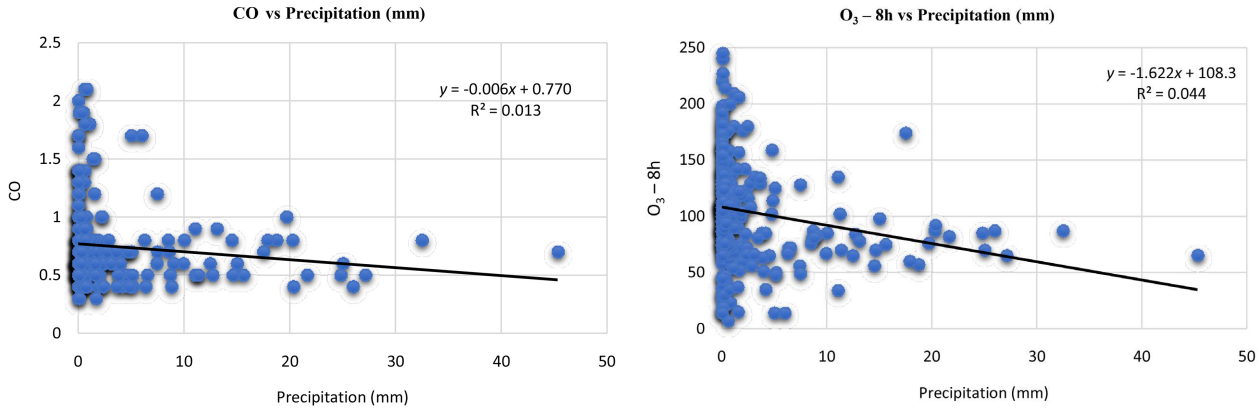

Figure 13. The relationship between air pollutants and precipitation before and during the COVID-19 period.

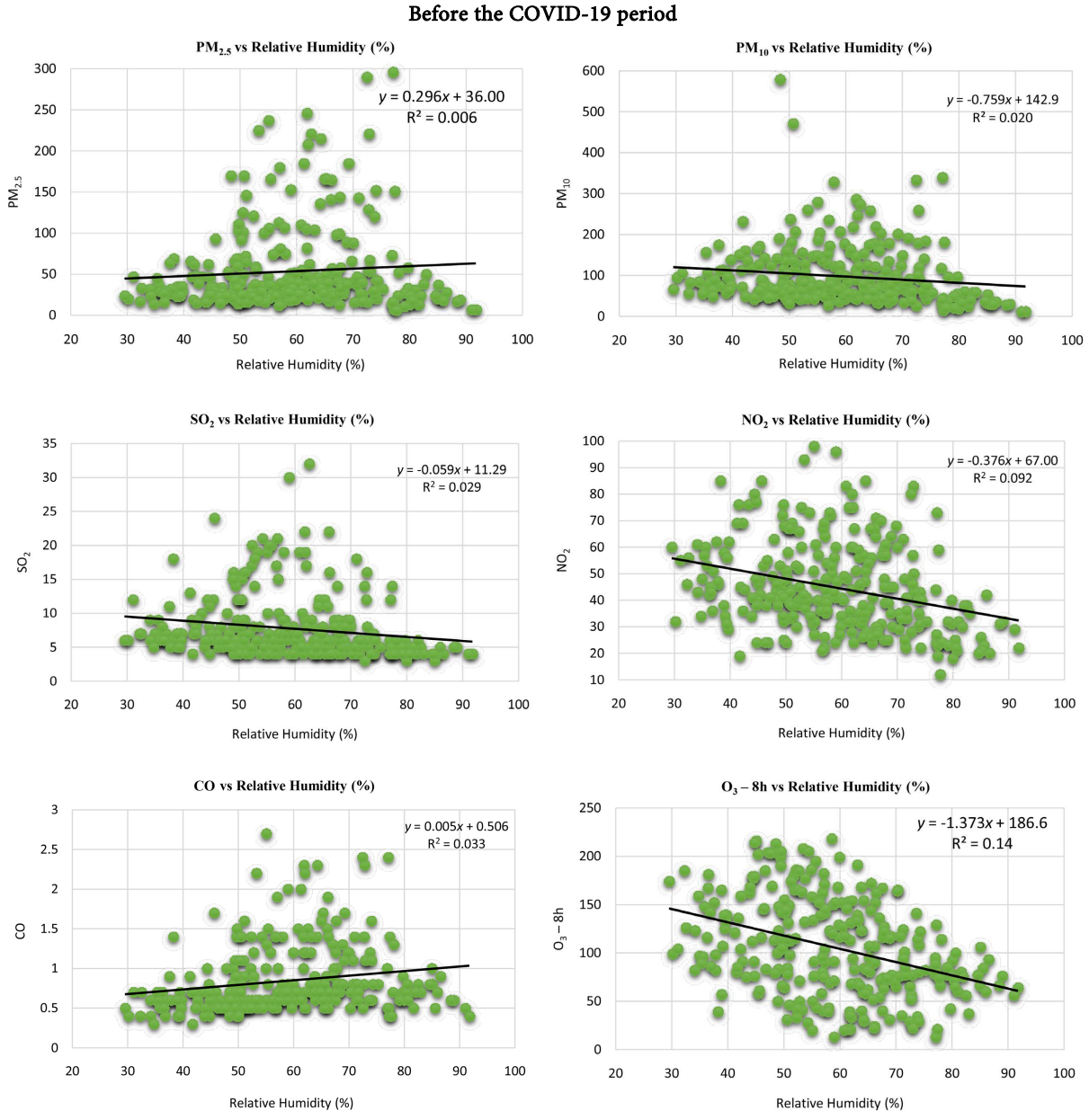

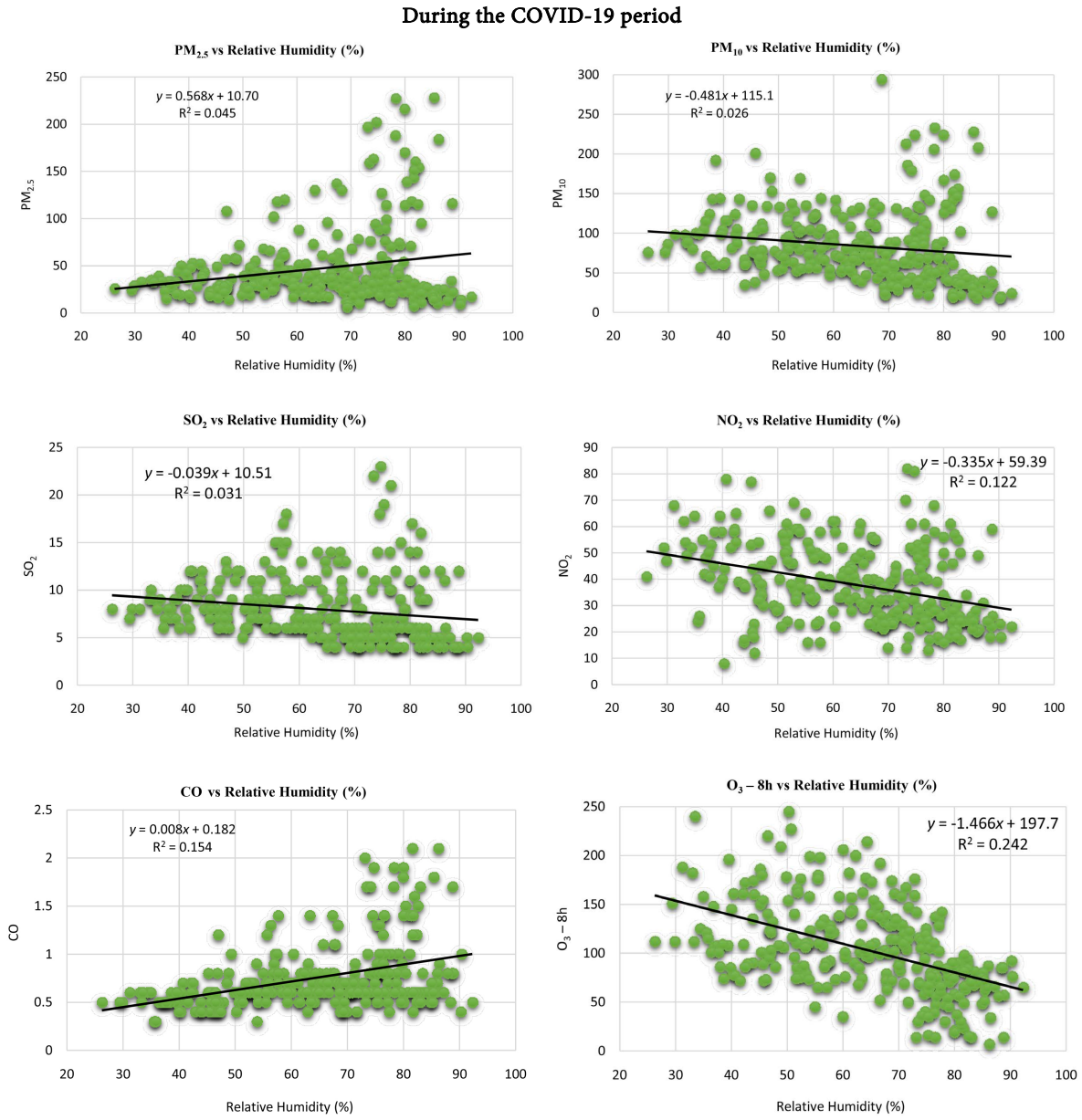

Figure 14. The relationship between air pollutants and relative humidity before and during the COVID-19 period.

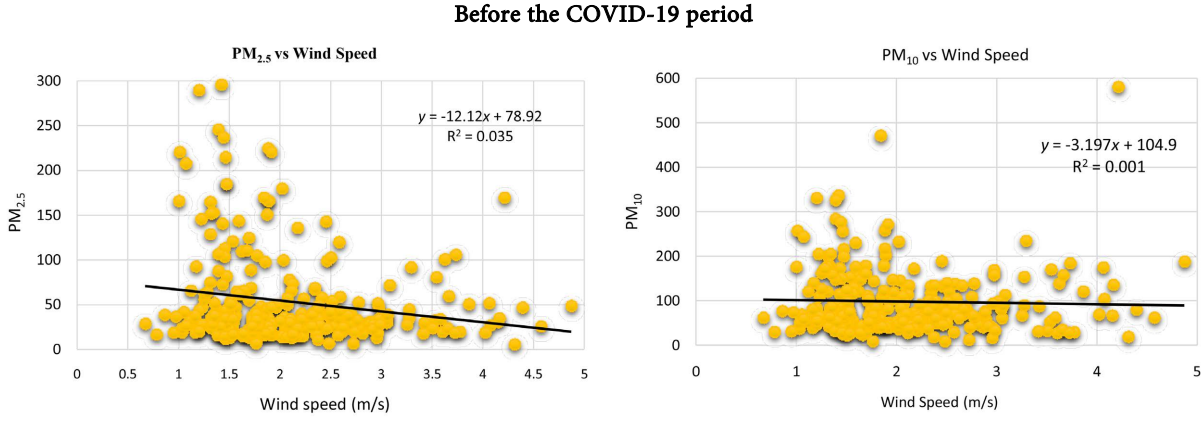

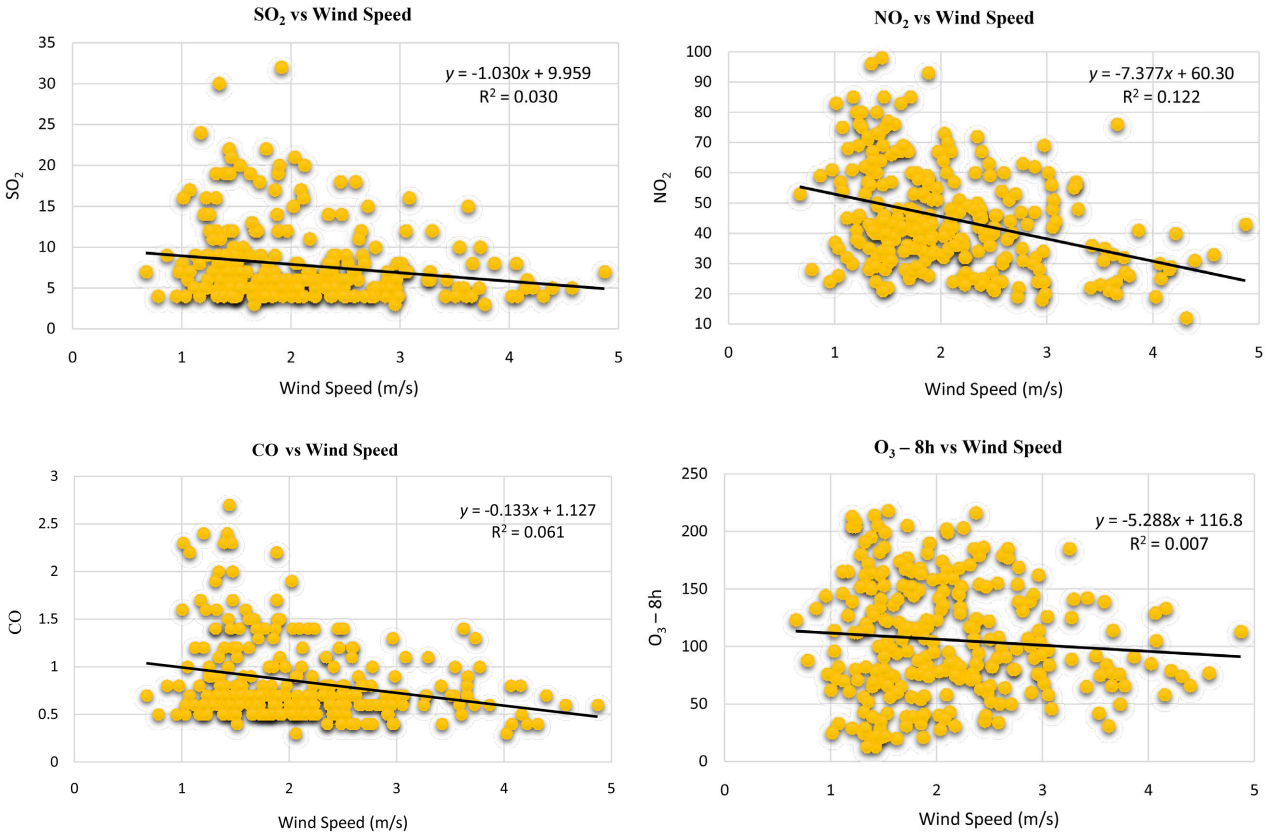

During the COVID-19 period

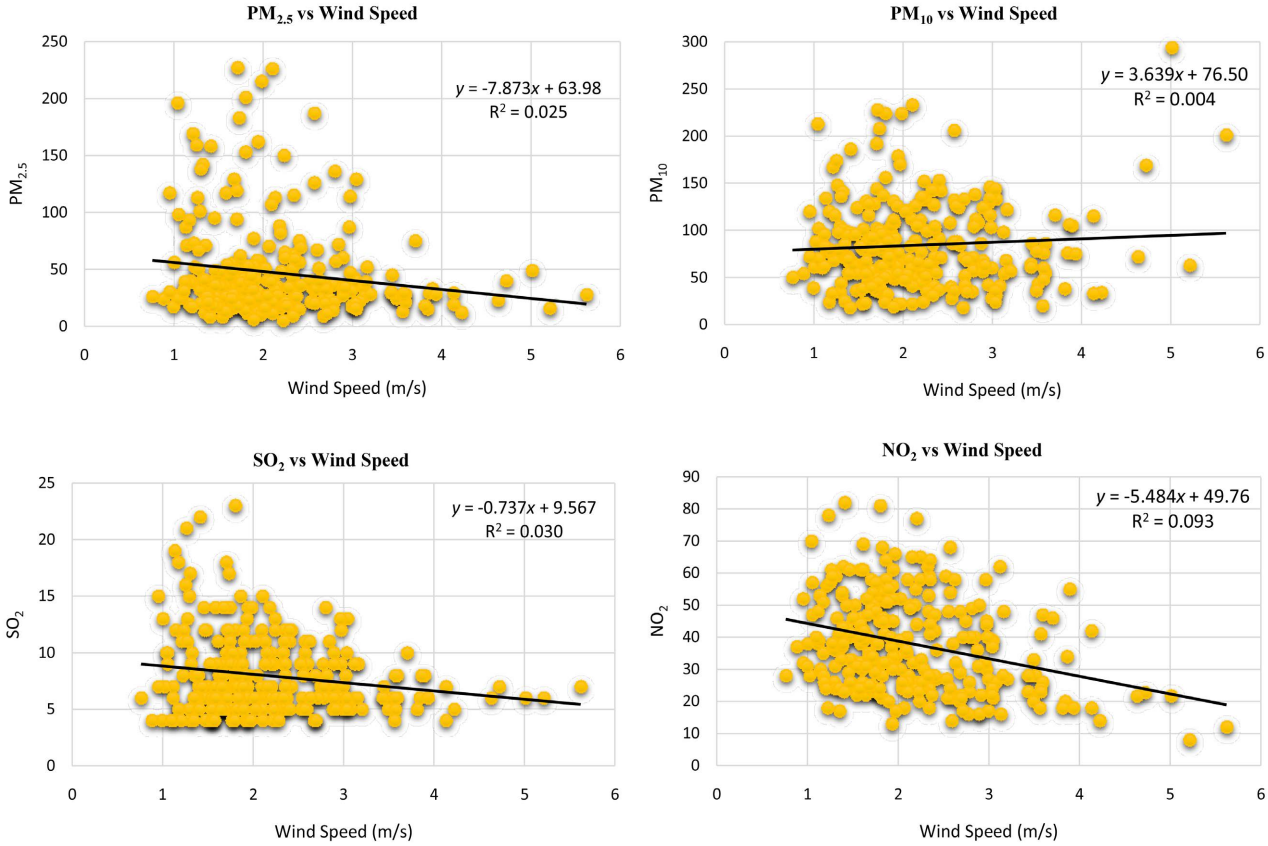

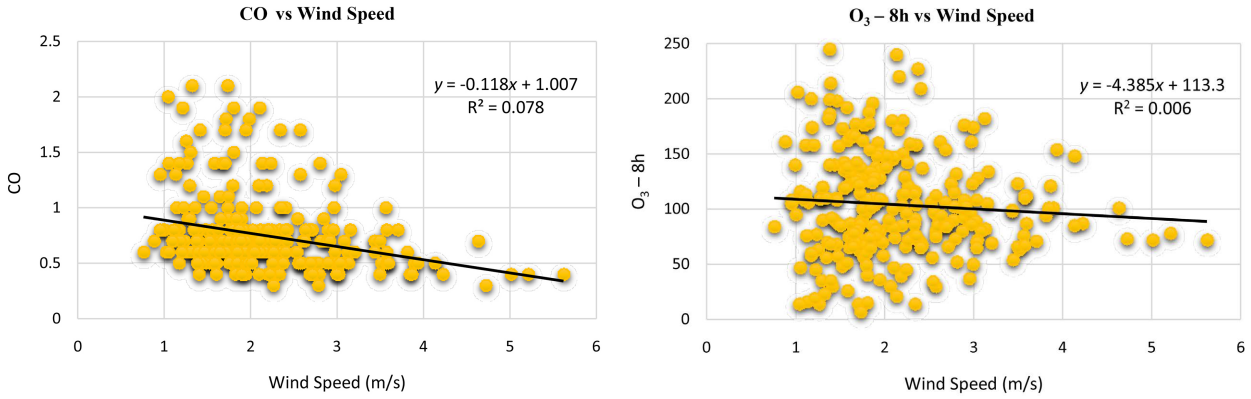

Figure 15. The relationship between air pollutants and wind speed before and during the COVID-19 period.

3.2.1. Air Pollutants and Temperature

A negative correlation was recorded between different air pollutants ($PM_{2.5}$, NO_2, PM_{10}, CO, and SO_2) and the temperature in 2019 with correlation coefficient (R2) values i.e. 0.4592, 0.234, 0.2853, 0.4867, 0.4342, respectively (**Figure 12**). These results reveal that air pollutants such as $PM_{2.5}$, NO_2, PM_{10}, CO, and SO_2 reduce when the temperature increases. However, a moderately positive correlation was recorded between O_3-8h and temperature during 2019. Its correlation coefficient value was R2 = 0.6344, which showed that O_3-8h in the air increases with an increase in temperature.

During the COVID-19 period in 2020, a negative correlation between different air pollutants ($PM_{2.5}$, NO_2, PM_{10}, CO, and SO_2) and temperature was recorded with R2 = 0.4269, 0.0264, 0.2251, 0.3359, 0.3815, respectively (**Figure 12**). These results display that the concentration of air pollutants such as $PM_{2.5}$, NO_2, PM_{10}, CO, and SO_2 decreased as the temperature increased. However, a moderately positive correlation (R2 = 0.4411) between O_3-8h and temperature was observed during 2020, which showed that the O_3-8h in ambient air escalates with increasing temperature.

Comparing the correlation results between air pollutants and temperature before and during COVID-19, the R2 values were lower than during COVID-19. It has been found that the unpropitious impact of environmental ozone pollution on humans' well-being increases with increasing temperature (Jacob & Winner, 2009). The natural cover of an urban environment composed of wetlands, vegetation, waterbody, bare soil, and open spaces is usually substituted by the characteristics of diverse land-use types, such as roads, sidewalks, buildings, and other artificial structures made of different materials (such as asphalt), metals and bricks, which themselves can absorb heat during the day and then release heat at night; All these together lead to the rise of surface temperature in an urban environment, which in turn contributes to the development of Urban Heat Island (UHI) phenomenon (Ayanlade, 2016; Oke, 1973; Sampson et al., 2021) and it supports the increase in air pollution. Jiang et al. (2020) conducted a similar study in Fuzhou, China, and recorded similar results i.e. the temperature was negatively correlated with PM_{10}, $PM_{2.5}$, and NO_2 and positively correlated with

O_3-8h.

3.2.2. Air Pollutants and Precipitation

Figure 13 shows a weak negative correlation between air pollutants i.e. $PM_{2.5}$, NO_2, PM_{10}, CO, SO_2, and O_3-8h, and the precipitation before and during COVID-19. These results show that air pollutants such as $PM_{2.5}$, NO_2, PM_{10}, CO, SO_2, and O_3-8h increase as the precipitation decreases. However, this reduction is the same in magnitude as that detected during a similar time during the period of COVID-19 in this study. Moreover, the values of R2 during the COVID-19 period were lower than before the COVID-19 period. Earlier, it has been found that precipitation can have a variable effect on air pollutants by removing gaseous pollution and particulate matter deposition through atmospheric chemical processes (Shukla et al., 2008). Similarly, Liu et al. (2020) pointed out that the exclusion impact of precipitation on aerosol particles was associated with raindrop diameter, aerosol particle size, and precipitation intensity. They suggested that air pollutants may not be correlated with precipitation.

3.2.3. Air Pollutants and Relative Humidity

Air pollutants such as PM_{10}, NO_2, SO_2, and O_3-8h were negatively correlated with relative humidity before and during COVID-19 (**Figure 14**). These results show that the concentration of air pollutants such as PM_{10}, NO_2, SO_2, and O_3-8h decreases with increasing relative humidity. Kayes et al., (2019) found that the concentration of most air pollutants had a negative relationship with relative humidity. Relative humidity affects the movement of particles and may deposit particles on the ground surface. Consequently, air pollutants decrease with the rise in relative humidity (Giri et al., 2008; Kumar, 2020). A weak but positive correlation between $PM_{2.5}$, CO, and relative humidity was recorded before and during COVID-19.

3.2.4. Air Pollutants and Wind Speed

A weak and negative correlation between air pollutants ($PM_{2.5}$, NO_2, SO_2, CO, and O_3-8h) and wind speed was recorded before and during the COVID-19 period in the study area (**Figure 15**). These results showed that air pollutants such as $PM_{2.5}$, NO_2, SO_2, CO, and O_3-8h increase as the wind speed decreases. The wind significantly impacts pollution (Liu et al., 2020). Dincer et al., (2010) mentioned that wind speed negatively correlates with the concentration of air pollutants data. However, in this study, PM_{10} and wind speed have shown a weak but positive correlation during COVID-19. The relationship between air pollutants and wind speed can supply significant details about air pollution, as wind speeds can move air pollutants from distant sources (Dincer et al., 2010).

The densely populated capital of the Shanxi province of Xi'an had the highest air pollutant emissions before the COVID-19 period. However, activities of air pollutant emission sources, such as houses, coal-based thermal power plants, residential biomass burning, industries (sulfur-contained fuel used in different industries), and construction activities, were reduced during COVID-19. As a

result, the correlation coefficient values regarding various parameters studies decreased during the COVID-19 period compared to before the COVID-19 period.

4. Conclusions and Recommendations

The COVID-19 pandemic (SARS-COV-2) has led to an improvement in global air quality. This study investigated the spatial distribution pattern of air pollutants, the temporal distribution of air quality indices, and the trends in air pollutant patterns. Finally, it analyzed the relationship between meteorological indicators (temperature, precipitation, humidity, and wind speed) and air pollutants (PM_{10}, NO_2, $PM_{2.5}$, CO, SO_2, and O_3-8h), in Xi'an, China, before and during the COVID-19 period. Based on the experimental analyses, this study concluded that the concentration of air pollutants such as $PM_{2.5}$, NO_2, PM_{10}, CO, and SO_2 decreases in winter, spring, and summer. In contrast, the concentration of O_3-8h increases from winter to summer due to the variation in weather conditions during COVID-19. No severely polluted days were reported during COVID-19, and the air quality index decreased by 100 percent. A significant trend was identified in air pollutants ($PM_{2.5}$, PM_{10}, and CO), while no significant trend was observed in the case of O_3-8h, NO_2, and SO_2 before COVID-19.

The results recorded in this study will help recognize Xi'an's air pollution during and before COVID-19. The results may also provide helpful evidence of the benefits of different air pollution control approaches before and during COVID-19. In addition, these analyses are an addition to identifying the literature before and during the impact of COVID-19 on air pollution and, more generally, identifying air quality changes related to specific causes. In this study, outcomes provide information for further research to categorize the status of exposure performance and level of air pollution, particularly from the studies with the robust procedure usual for essential confounders. The advantages of air quality measures during the COVID-19 lockdown were performed to be an inimitable chance for pollution control strategies. Finally, this study would aid in various clean air programs and air pollution modeling in the future globally.

Acknowledgements

This research was funded by the Postdoctoral Startup Research Fund of Henan University, number (CJ3050A0671293).

Conflicts of Interest

The authors declare no conflicts of interest regarding the publication of this paper.

References

Abdullah, S., Mansor, A. A., Napi, N. N. L. M., Mansor, W. N. W., Ahmed, A. N., Ismail, M. et al. (2020). Air Quality Status during 2020 Malaysia Movement Control Order (MCO) Due to 2019 Novel Coronavirus (2019-Ncov) Pandemic. *Science of The Total*

Environment, 729, Article ID: 139022. https://doi.org/10.1016/j.scitotenv.2020.139022

Alqasemi, A. S., Hereher, M. E., Kaplan, G., Al-Quraishi, A. M. F., & Saibi, H. (2021). Impact of COVID-19 Lockdown Upon the Air Quality and Surface Urban Heat Island Intensity over the United Arab Emirates. *Science of The Total Environment, 767,* Article ID: 144330. https://doi.org/10.1016/j.scitotenv.2020.144330

Ayanlade, A. (2016). Variation in Diurnal and Seasonal Urban Land Surface Temperature: Landuse Change Impacts Assessment over Lagos Metropolitan City. *Modeling Earth Systems and Environment, 2,* 1-8. https://doi.org/10.1007/s40808-016-0238-z

Borhani, F., Shafiepour Motlagh, M., Stohl, A., Rashidi, Y., & Ehsani, A. H. (2021). Changes in Short-Lived Climate Pollutants during the COVID-19 Pandemic in Tehran, Iran. *Environmental Monitoring and Assessment, 193,* Article No. 331. https://doi.org/10.1007/s10661-021-09096-w

Cao, J., Cheng, Y., & Yu, C. (2018). Urban Air Quality Management in Xi'an. *Indoor and Built Environment, 27,* 3-6. https://doi.org/10.1177/1420326x17742007

Chen, B., Liang, H., Yuan, X., Hu, Y., Xu, M., Zhao, Y., Zhang, B., & Zhu, X. (2021). *Roles of Meteorological Conditions in COVID-19 Transmission on a Worldwide Scale*.

Chinazzi, M., Davis, J. T., Ajelli, M., Gioannini, C., Litvinova, M., Merler, S. et al. (2020). The Effect of Travel Restrictions on the Spread of the 2019 Novel Coronavirus (COVID-19) Outbreak. *Science, 368,* 395-400. https://doi.org/10.1126/science.aba9757

Chow, B. L., & Yeung, J. (2006). Scatter Diagram. In P. M. Swamidass (Ed.), *Encyclopedia of Production and Manufacturing Management* (2000 ed., pp. 43-54). Springer. https://link.springer.com/referenceworkentry/10.1007/1-4020-0612-8_843

Dai, Q., Bi, X., Liu, B., Li, L., Ding, J., Song, W. et al. (2018). Chemical Nature of $PM_{2.5}$ and PM_{10} in Xi'an, China: Insights into Primary Emissions and Secondary Particle Formation. *Environmental Pollution, 240,* 155-166. https://doi.org/10.1016/j.envpol.2018.04.111

Dhahad, H. A., Fayad, M. A., Chaichan, M. T., Abdulhady Jaber, A., & Megaritis, T. (2021). Influence of Fuel Injection Timing Strategies on Performance, Combustion, Emissions and Particulate Matter Characteristics Fueled with Rapeseed Methyl Ester in Modern Diesel Engine. *Fuel, 306,* Article ID: 121589. https://doi.org/10.1016/j.fuel.2021.121589

Dincer, I., Midilli, A., Hepbasli, A., & Karakoc, T. H. (2010). *Global Warming: Engineering Solutions (Green Energy and Technology)* (Vol. 31). Springer.

Feng, T., Bei, N., Huang, R., Cao, J., Zhang, Q., Zhou, W. et al. (2016). Summertime Ozone Formation in Xi'an and Surrounding Areas, China. *Atmospheric Chemistry and Physics, 16,* 4323-4342. https://doi.org/10.5194/acp-16-4323-2016

Giri, D., Murthy, K., & Adhikary, P. R. (2008). The Influence of Meteorological Conditions on PM_{10} Concentrations in Kathmandu Valley. *International Journal of Environmental Research, 2,* 49-60.

Gouda, K. C., Singh, P., P, N., Benke, M., Kumari, R., Agnihotri, G. et al. (2021). Assessment of Air Pollution Status during COVID-19 Lockdown (March-May 2020) over Bangalore City in India. *Environmental Monitoring and Assessment, 193,* Article No. 395. https://doi.org/10.1007/s10661-021-09177-w

Helsel, D. R., & Hirsch, R. M. (1992). *Statistical Methods in Water Resources*. Elsevier.

Islam, M. S., & Chowdhury, T. A. (2021). Effect of COVID-19 Pandemic-Induced Lockdown (General Holiday) on Air Quality of Dhaka City. *Environmental Monitoring and Assessment, 193,* Article No. 343. https://doi.org/10.1007/s10661-021-09120-z

Jacob, D. J., & Winner, D. A. (2009). Effect of Climate Change on Air Quality. *Atmos-*

pheric Environment, 43, 51-63. https://doi.org/10.1016/j.atmosenv.2008.09.051

Jahangiri, M., Jahangiri, M., & Najafgholipour, M. (2020). The Sensitivity and Specificity Analyses of Ambient Temperature and Population Size on the Transmission Rate of the Novel Coronavirus (COVID-19) in Different Provinces of Iran. *Science of the Total Environment, 728,* Article ID: 138872. https://doi.org/10.1016/j.scitotenv.2020.138872

Jensen, S. S., Berkowicz, R., Sten Hansen, H., & Hertel, O. (2001). A Danish Decision-Support GIS Tool for Management of Urban Air Quality and Human Exposures. *Transportation Research Part D: Transport and Environment, 6,* 229-241. https://doi.org/10.1016/s1361-9209(00)00026-2

Jiang, Y., Chen, J., Wu, C., Lin, X., Zhou, Q., Ji, S. et al. (2020). Temporal Cross-Correlations between Air Pollutants and Outpatient Visits for Respiratory and Circulatory System Diseases in Fuzhou, China. *BMC Public Health, 20,* Article No. 1131. https://doi.org/10.1186/s12889-020-08915-y

Kayes, I., Shahriar, S. A., Hasan, K., Akhter, M., Kabir, M. M., & Salam, M. A. (2019). The Relationships between Meteorological Parameters and Air Pollutants in an Urban Environment. *Global Journal of Environmental Science and Management, 5,* 265-278.

Kerimray, A., Baimatova, N., Ibragimova, O. P., Bukenov, B., Kenessov, B., Plotitsyn, P. et al. (2020). Assessing Air Quality Changes in Large Cities during COVID-19 Lockdowns: The Impacts of Traffic-Free Urban Conditions in Almaty, Kazakhstan. *Science of the Total Environment, 730,* Article ID: 139179. https://doi.org/10.1016/j.scitotenv.2020.139179

Khorsandi, B., Farzad, K., Tahriri, H., & Maknoon, R. (2021). Association between Short-Term Exposure to Air Pollution and COVID-19 Hospital Admission/Mortality during Warm Seasons. *Environmental Monitoring and Assessment, 193,* Article No. 426. https://doi.org/10.1007/s10661-021-09210-y

Kraemer, M. U. G., Yang, C., Gutierrez, B., Wu, C., Klein, B., Pigott, D. M. et al. (2020). The Effect of Human Mobility and Control Measures on the COVID-19 Epidemic in China. *Science, 368,* 493-497. https://doi.org/10.1126/science.abb4218

Kumar, A., Gupta, I., Brandt, J., Kumar, R., Dikshit, A. K., & Patil, R. S. (2016). Air Quality Mapping Using GIS and Economic Evaluation of Health Impact for Mumbai City, India. *Journal of the Air & Waste Management Association, 66,* 470-481. https://doi.org/10.1080/10962247.2016.1143887

Kumar, S. (2020). Effect of Meteorological Parameters on Spread of COVID-19 in India and Air Quality during Lockdown. *Science of The Total Environment, 745,* Article ID: 141021. https://doi.org/10.1016/j.scitotenv.2020.141021

Kumari, P., & Toshniwal, D. (2020). Impact of Lockdown on Air Quality over Major Cities across the Globe during COVID-19 Pandemic. *Urban Climate, 34,* Article ID: 100719. https://doi.org/10.1016/j.uclim.2020.100719

Latif, M. T., Dominick, D., Hawari, N. S. S. L., Mohtar, A. A. A., & Othman, M. (2021). The Concentration of Major Air Pollutants during the Movement Control Order Due to the COVID-19 Pandemic in the Klang Valley, Malaysia. *Sustainable Cities and Society, 66,* Article ID: 102660. https://doi.org/10.1016/j.scs.2020.102660

Li, L., Li, Q., Huang, L., Wang, Q., Zhu, A., Xu, J. et al. (2020). Air Quality Changes during the COVID-19 Lockdown over the Yangtze River Delta Region: An Insight into the Impact of Human Activity Pattern Changes on Air Pollution Variation. *Science of the Total Environment, 732,* Article ID: 139282. https://doi.org/10.1016/j.scitotenv.2020.139282

Li, N., He, Q., Greenberg, J., Guenther, A., Li, J., Cao, J. et al. (2018). Impacts of Biogenic and Anthropogenic Emissions on Summertime Ozone Formation in the Guanzhong

Basin, China. *Atmospheric Chemistry and Physics, 18,* 7489-7507. https://doi.org/10.5194/acp-18-7489-2018

Liu, F., Wang, M., & Zheng, M. (2021). Effects of COVID-19 Lockdown on Global Air Quality and Health. *Science of The Total Environment, 755,* Article ID: 142533. https://doi.org/10.1016/j.scitotenv.2020.142533

Liu, J., Zhou, J., Yao, J., Zhang, X., Li, L., Xu, X. et al. (2020). Impact of Meteorological Factors on the COVID-19 Transmission: A Multi-City Study in China. *Science of the Total Environment, 726,* Article ID: 138513. https://doi.org/10.1016/j.scitotenv.2020.138513

Liu, Q., Harris, J. T., Chiu, L. S., Sun, D., Houser, P. R., Yu, M. et al. (2021). Spatiotemporal Impacts of COVID-19 on Air Pollution in California, USA. *Science of The Total Environment, 750,* Article ID: 141592. https://doi.org/10.1016/j.scitotenv.2020.141592

Liu, Z., Shen, L., Yan, C., Du, J., Li, Y., & Zhao, H. (2020). Analysis of the Influence of Precipitation and Wind on $PM_{2.5}$ and PM_{10} in the Atmosphere. *Advances in Meteorology, 2020,* Article ID: 5039613. https://doi.org/10.1155/2020/5039613

Ma, Y., Zhao, Y., Liu, J., He, X., Wang, B., Fu, S. et al. (2020). Effects of Temperature Variation and Humidity on the Death of COVID-19 in Wuhan, China. *Science of the Total Environment, 724,* Article ID: 138226. https://doi.org/10.1016/j.scitotenv.2020.138226

Mahato, S., Pal, S., & Ghosh, K. G. (2020). Effect of Lockdown amid COVID-19 Pandemic on Air Quality of the Megacity Delhi, India. *Science of the Total Environment, 730,* Article ID: 139086. https://doi.org/10.1016/j.scitotenv.2020.139086

Manju, A., Kalaiselvi, K., Dhananjayan, V., Palanivel, M., Banupriya, G. S., Vidhya, M. H. et al. (2018). Spatio-Seasonal Variation in Ambient Air Pollutants and Influence of Meteorological Factors in Coimbatore, Southern India. *Air Quality, Atmosphere & Health, 11,* 1179-1189. https://doi.org/10.1007/s11869-018-0617-x

Meals, D. W., Spooner, J., Dressing, S. A., & Harcum, J. B. (2011). *Statistical Analysis for Monotonic Trends*.

Mehmood, K., Bao, Y., Abrar, M. M., Petropoulos, G. P., Saifullah, Soban, A. et al. (2021). Spatiotemporal Variability of COVID-19 Pandemic in Relation to Air Pollution, Climate and Socioeconomic Factors in Pakistan. *Chemosphere, 271,* Article ID: 129584. https://doi.org/10.1016/j.chemosphere.2021.129584

Mokoena, K. K., Ethan, C. J., Yu, Y., Shale, K., & Liu, F. (2019). Ambient Air Pollution and Respiratory Mortality in Xi'an, China: A Time-Series Analysis. *Respiratory Research, 20,* Article No. 139. https://doi.org/10.1186/s12931-019-1117-8

Mor, S., Kumar, S., Singh, T., Dogra, S., Pandey, V., & Ravindra, K. (2021). Impact of COVID-19 Lockdown on Air Quality in Chandigarh, India: Understanding the Emission Sources during Controlled Anthropogenic Activities. *Chemosphere, 263,* Article ID: 127978. https://doi.org/10.1016/j.chemosphere.2020.127978

Oke, T. R. (1973). City Size and the Urban Heat Island. *Atmospheric Environment (1967), 7,* 769-779. https://doi.org/10.1016/0004-6981(73)90140-6

Pomponi, F., Li, M., Sun, Y., Malik, A., Lenzen, M., Fountas, G. et al. (2020). A Novel Method for Estimating Emissions Reductions Caused by the Restriction of Mobility: The Case of the COVID-19 Pandemic. *Environmental Science & Technology Letters, 8,* 46-52. https://doi.org/10.1021/acs.estlett.0c00764

Radaideh, J. A. (2017). Effect of Meteorological Variables on Air Pollutants Variation in Arid Climates. *Journal of Environmental & Analytical Toxicology, 7,* Article ID: 1000478. https://doi.org/10.4172/2161-0525.1000478

Rahman, M. S., Azad, M. A. K., Hasanuzzaman, M., Salam, R., Islam, A. R. M. T., Rahman, M. M. et al. (2021). How Air Quality and COVID-19 Transmission Change under Different Lockdown Scenarios? A Case from Dhaka City, Bangladesh. *Science of the Total Environment, 762,* Article ID: 143161. https://doi.org/10.1016/j.scitotenv.2020.143161

Raza, A., Khan, M. T. I., Ali, Q., Hussain, T., & Narjis, S. (2021). Association between Meteorological Indicators and COVID-19 Pandemic in Pakistan. *Environmental Science and Pollution Research, 28,* 40378-40393. https://doi.org/10.1007/s11356-020-11203-2

Sampson, A. P., Weli, V. E., Nwagbara, M. O., & Eludoyin, O. S. (2021). Sensations of Air Temperature Variability and Mitigation Strategies in Urban Environments. *Journal of Human, Earth, and Future, 2,* 100-113. https://doi.org/10.28991/hef-2021-02-02-02

Shi, P., Dong, Y., Yan, H., Zhao, C., Li, X., Liu, W. et al. (2020). Impact of Temperature on the Dynamics of the COVID-19 Outbreak in China. *Science of the Total Environment, 728,* Article ID: 138890. https://doi.org/10.1016/j.scitotenv.2020.138890

Shukla, J. B., Misra, A. K., Sundar, S., & Naresh, R. (2008). Effect of Rain on Removal of a Gaseous Pollutant and Two Different Particulate Matters from the Atmosphere of a City. *Mathematical and Computer Modelling, 48,* 832-844. https://doi.org/10.1016/j.mcm.2007.10.016

Singh, V., Singh, S., Biswal, A., Kesarkar, A. P., Mor, S., & Ravindra, K. (2020). Diurnal and Temporal Changes in Air Pollution during COVID-19 Strict Lockdown over Different Regions of India. *Environmental Pollution, 266,* 115368. https://doi.org/10.1016/j.envpol.2020.115368

Sun, C., & Zhai, Z. (2020). The Efficacy of Social Distance and Ventilation Effectiveness in Preventing COVID-19 Transmission. *Sustainable Cities and Society, 62,* Article ID: 102390. https://doi.org/10.1016/j.scs.2020.102390

Tang, B., Wang, X., Li, Q., Bragazzi, N. L., Tang, S., Xiao, Y. et al. (2020). Estimation of the Transmission Risk of the 2019-Ncov and Its Implication for Public Health Interventions. *Journal of Clinical Medicine, 9,* Article No. 462. https://doi.org/10.3390/jcm9020462

Tanzer-Gruener, R., Li, J., Eilenberg, S. R., Robinson, A. L., & Presto, A. A. (2020). Impacts of Modifiable Factors on Ambient Air Pollution: A Case Study of COVID-19 Shutdowns. *Environmental Science & Technology Letters, 7,* 554-559. https://doi.org/10.1021/acs.estlett.0c00365

Tian, H., Liu, Y., Li, Y., Wu, C., Chen, B., Kraemer, M. U. G. et al. (2020). An Investigation of Transmission Control Measures during the First 50 Days of the COVID-19 Epidemic in China. *Science, 368,* 638-642. https://doi.org/10.1126/science.abb6105

Tosepu, R., Gunawan, J., Effendy, D. S., Ahmad, L. O. A. I., Lestari, H., Bahar, H. et al. (2020). Correlation between Weather and Covid-19 Pandemic in Jakarta, Indonesia. *Science of the Total Environment, 725,* Article ID: 138436. https://doi.org/10.1016/j.scitotenv.2020.138436

van Wijk, J. J., & van Selow, E. R. (1999, October 25). Cluster and Calendar Based Visualization of Time Series Data. In *The IEEE Symposium on Information Visualization* (pp. 4-9). IEEE.

Wang, D., Hu, J., Xu, Y., Lv, D., Xie, X., Kleeman, M. et al. (2014). Source Contributions to Primary and Secondary Inorganic Particulate Matter during a Severe Wintertime $PM_{2.5}$ Pollution Episode in Xi'an, China. *Atmospheric Environment, 97,* 182-194. https://doi.org/10.1016/j.atmosenv.2014.08.020

Wang, Q., & Su, M. (2020). A Preliminary Assessment of the Impact of COVID-19 on

Environment—A Case Study of China. *Science of the Total Environment, 728,* Article ID: 138915. https://doi.org/10.1016/j.scitotenv.2020.138915

Wang, Y., Li, S., Wang, M., Sun, H., Mu, Z., Zhang, L. et al. (2019). Source Apportionment of Environmentally Persistent Free Radicals (EPFRs) in $PM_{2.5}$ over Xi'an, China. *Science of the Total Environment, 689,* 193-202. https://doi.org/10.1016/j.scitotenv.2019.06.424

Wang, Y., Wang, M., Li, S., Sun, H., Mu, Z., Zhang, L. et al. (2020a). Study on the Oxidation Potential of the Water-Soluble Components of Ambient $PM_{2.5}$ over Xi'an, China: Pollution Levels, Source Apportionment and Transport Pathways. *Environment International, 136,* Article ID: 105515. https://doi.org/10.1016/j.envint.2020.105515

Wang, Y., Yuan, Y., Wang, Q., Liu, C., Zhi, Q., & Cao, J. (2020b). Changes in Air Quality Related to the Control of Coronavirus in China: Implications for Traffic and Industrial Emissions. *Science of the Total Environment, 731,* Article ID: 139133. https://doi.org/10.1016/j.scitotenv.2020.139133

WHO (2016). *Ambient Air Pollution: A Global Assessment of Exposure and Burden of Disease*.

WHO (2021). *Xian Air Quality Index (AQI) and China Air Pollution*. https://www.iqair.com/china/shaanxi/xian

Wyche, K. P., Nichols, M., Parfitt, H., Beckett, P., Gregg, D. J., Smallbone, K. L. et al. (2021). Changes in Ambient Air Quality and Atmospheric Composition and Reactivity in the South East of the UK as a Result of the COVID-19 Lockdown. *Science of the Total Environment, 755,* Article ID: 142526. https://doi.org/10.1016/j.scitotenv.2020.142526

Yang, M., Fan, H., & Zhao, K. (2020). Fine-Grained Spatiotemporal Analysis of the Impact of Restricting Factories, Motor Vehicles, and Fireworks on Air Pollution. *International Journal of Environmental Research and Public Health, 17,* Article No. 4828. https://doi.org/10.3390/ijerph17134828

Yao, L., Li, W., & Du, Y. (2021). Impact of COVID-19 on Air Quality in the Yangtze River Delta, China. *Environmental Monitoring and Assessment, 193,* Article No. 523. https://doi.org/10.1007/s10661-021-09342-1

Yuan, Q., Qi, B., Hu, D., Wang, J., Zhang, J., Yang, H. et al. (2021). Spatiotemporal Variations and Reduction of Air Pollutants during the COVID-19 Pandemic in a Megacity of Yangtze River Delta in China. *Science of the Total Environment, 751,* Article ID: 141820. https://doi.org/10.1016/j.scitotenv.2020.141820

List of Abbreviations

Particulate Matter (PM), Nitrogen Dioxide (NO_2), Carbon Monoxide (CO), Sulfur Dioxide SO_2, Ozone O_3, Air Quality Index (AQI), Volatile Organic Compounds (VOC), Nitrogen Oxide (NO_x), particulate matter (PM), National Aeronautics and Space Administration (NASA), Prediction of Worldwide Energy Resources (POWER), Standard Deviation (SD), Geographic Information System (GIS).